91602
new 82-10

ontario hydro
research division

COMPLIMENTARY COPY
Please Credit Ontario Hydro Research if
Reproduced in Whole or in Part

LATERAL LOAD BEHAVIOUR OF DRILLED PIERS IN LEDA CLAY

Report No 87-19-K

H.S. Radhakrishna and R. Tsang
Engineers
Soil Sciences Section
Civil Research Department

ABSTRACT

Ultimate load and deflection behaviour of laterally loaded drilled piers in soft clay were investigated by a field program of load testing full scale footings. The methods of construction used and the behaviour of the footings under shear and moment loads simulating the lattice type and steel pole structures are described. The effect of depth to diameter ratio and moment to shear ratio on the deflection and rotation of the piers is discussed. The measured responses are compared with theoretical predictions made by a non-linear, four spring model (PADLL Program) developed by EPRI. Implications of the findings for the design of drilled shafts for steel poles in Leda clay are also discussed.

job	file	date	report no.
43-135-431	843.2	September 24, 1987	87-19-K

TABLE OF CONTENTS

	Page
INTRODUCTION	1
SOIL PROPERTIES	2
TEST FOUNDATIONS	2
CONSTRUCTION OF FOOTINGS	2
Soil Disturbance	3
TEST ARRANGEMENT	3
INSTRUMENTATION	4
TEST RESULTS	4
ANALYSIS OF TEST DATA	4
Measured Load-Deflection Response	5
Prediction by Theoretical Model	5
Comparison Between Predicted and Measured Reponses of Test Footings	7
Footings With No Overturning Moment	7
Moment Footings	8
Footing Deflection and Soil Pressure Distribution	9
DESIGN CONSIDERATIONS	10
CONCLUSIONS	12
ACKNOWLEDGEMENTS	13
REFERENCES	15
TABLES I to XIII	16
FIGURES 1 to 42	17
APPENDIX A	70
APPENDIX B	75
DISTRIBUTION	last page

ontario hydro
research division

To Mr. B.A. Oliver
Group Manager, S&T Design
Design and Development Division

Attn: Mr. A.R. Collins

LATERAL LOAD BEHAVIOUR OF DRILLED SHAFTS IN A SENSITIVE CLAY

INTRODUCTION

Steel pole structures are used increasingly by electrical utilities to improve appearance and compactness of the transmission corridor for urban areas. Drilled piers are the most commonly used foundations for steel poles. The steel pole foundations are required to resist a large overturning moment coupled with some shear and vertical loads induced by wind forces on the conductor and pole structure.

Drilled piers have been successfully used in competent soils such as sand, clay and glacial till deposits. However, the experience of designing and constructing large piers in soft and sensitive clay is limited. Since the straight sided drilled piers derive their lateral support from the strength and stiffness of the surrounding soil, the effects of construction disturbances in sensitive clay can significantly influence the performance of the foundations.

Ontario Hydro's proposed 500 kV transmission line in Eastern Ontario traverses through areas covered by the marine clay deposits of the ancient Champlain Sea, known as 'Leda clay'. This clay because of its metastable internal structure, exhibits high sensitivity due to disturbance, often resulting in a significant loss of strength and greatly increased deformations (Crawford 1968). While the geotechnical properties of this clay are well researched (Crawford and Eden, 1965, Law et al, 1977), the lateral load behaviour of drilled piers in sensitive clay is not well understood.

A load test program was carried out by installing eleven fully instrumented full scale foundations in Leda clay at the Gloucester test site near Ottawa (Figure 1). The results of uplift and compression tests are presented in a separate report (Cragg and Radhakrishna, 1986). This report presents the results of the lateral shear and overturning moment tests under short-term loading conditions. The influence of construction disturbance, the foundation depth to diameter ratio and the moment to shear ratio were investigated. The test results are compared with theoretical predictions made by the computer code "Pier Analysis and Design for Lateral Loads" (PADLL) (Davidson, 1982).

SOIL PROPERTIES

The test site is located on marine deposits of the Champlain Sea about 10 km south of Ottawa, in Ontario, Canada. The geotechnical properties of the deposit and the soil stratigraphy as determined by in situ tests such as vane shear, dilatometer, piezocone and pressuremeter tests are summarized in Figure 2.

The soil deposit over the test site is relatively uniform. Beneath the topsoil, a sandy silt layer of 1.5 m thickness is encountered containing some decayed roots and woody material. The underlying grey silty clay deposit, which extends to a depth of 18 m, has four distinct zones identified by water content, Atterberg limits and preconsolidation pressure profiles. Undrained shear strength values for the clay vary between 20 and 30 kPa over the depth of the test footings (6.4 to 10 m). The sensitivity of this clay ranges from 3 to 8. The sandy silt layer at the top is considerably stronger than the clay deposit. The ground water table was near the ground surface and the site is fairly flat with poor drainage. The undrained shear strength and deformation modulus values determined by in situ and laboratory tests are summarized in Figures 3 and 4.

TEST FOUNDATIONS

Individual footing dimensions are summarized in Table I. Of the eleven drilled piers installed, three (Footings 1, 2 and 3) were tested under lateral load at ground level without overturning moment (to simulate the loading conditions of a lattice type tower footing). These footings were also tested in uplift/compression prior to lateral load testing.

Footings 6, 7 and 8 were constructed and tested in such a way as to simulate the loading conditions for a steel pole foundation. These concrete footings were extended above the ground level by about 3 m and were tested in pairs to develop the required moment and shear loading at the ground level (Figure 5). The embedment depth of these piers below grade ranged from 6.63 m to 12.73 m (Table I). The depth and diameter combinations of these 3 footings were selected so that the influence of the depth to diameter ratios of the drilled piers could be investigated.

CONSTRUCTION OF FOOTINGS

Considerable uncertainty surrounded the choice of an appropriate construction method due to the tendency for Leda clay to collapse into a liquid when disturbed. On a previous transmission line in Leda clay, conventional foundation augering had liquefied the natural clay within the footing dimensions and the clay slurry had to be displaced by the tremie concrete technique. Construction tests in similar soils were carried out in Norway by removing the native clay and maintaining the excavation open with a slurry of bentonite or water and fly ash or by water alone. The bentonite slurry was found to leave a thick smear on the sides of the concrete pier and reduced the side friction (DiBagio, 1985).

In this program, different methods of excavating and supporting the hole were tested. These consisted of augering and removal of the clay with screw augers and a bailing bucket. Welding a few cleats on the auger flights, to prevent the excavated clay from slipping back into the hole, was successful (Figure 6) and most of the test footings were constructed by this dry augering technique. A temporary steel liner was used to support the surface layer of silt and fill material. This resulted in an enlarged diameter of the footing by 4 to 20 cm in the top 1.5 to 3.2 m length of the footing.

Soil Disturbance

Disturbance to the clay was minimized by corkscrewing the auger into the ground, penetrating 0.3 to 0.6 m, and then rotating it a few turns to shear the clay on the augers from the surrounding soil. Removal of the excavated clay by lifting the augers often produced a large suction force which could cause basal heave or failure of the footing excavation at great depth. It was envisaged to provide vents in the auger flights to prevent large suction forces from developing when the auger was withdrawn from the holes. However, this was not needed as most of the augered holes did not show base failure. Static cone tests, performed through the footings showed no noticeable change in soil strength from before to after construction.

Except for a thin layer of remoulded clay smear, the sides of the hole were judged to be undisturbed. No significant lateral squeezing or caving of the holes was observed (Figures 7 and 8). In the case of the 16 m deep by 2.7 m diameter hole, some sloughing off of the clay below the cased section was observed when the hole was left unsupported for 4 hours.

A concrete pump was used to fill the augered holes with concrete, because its small diameter discharge pipe was able to fit through the instrumentation mounted on the reinforcing cage.

It was feared that the concrete exiting the discharge end of the pump at high velocity would disturb the clay at the bottom of the augered hole. To offset this effect, the initial cubic metre of concrete was placed slowly before a fast pumping rate was used, so as to form a protective cushion for the weak soil below. Records of the concrete volume poured into each footing versus the volume of soil excavated suggested that no basal bulbs were formed by pumping concrete.

TEST ARRANGEMENT

The footings were tested in pairs by using one of them as the reaction for the other. Footings 1, 2 and 3 were laterally loaded by means of a hydraulic jack and a steel strut positioned between the pair of footings, as shown in Figures 9 and 10. The overturning moment loading of Footings 6, 7 and 8 was achieved by pulling two footings together at the top while applying a thrust at ground level as shown in Figures 11 and 12. By adjusting the top and bottom loads, the desired moment to shear ratios were achieved. This loading arrangement allowed the simulation of the large

moment to shear ratios experienced by steel pole foundations. Typically an eccentricity of 20 to 30 m was employed in these tests. The top and bottom loads were applied simultaneously to maintain the moment to shear ratio.

INSTRUMENTATION

The principal measurements to be made in lateral load tests of drilled piers are the applied loads, the rotation and ground line deflections of the pier. The applied loads were monitored by means of load cells in tandem with the hydraulic jacks. The ground line deflections of the test piers were monitored by an LVDT mounted on a remotely supported batter board (Figure 13). Dial gauges and surveying measurements were used as back-up for the LVDT system. The rotation of the pier at the ground level was monitored by a tilt meter mounted on the pier (Figure 14).

In addition to the measurements made at the ground surface, the rotation and bending of the pier below the ground surface was monitored by means of a slope indicator probe which was lowered into a special casing embedded in the concrete pier (Figure 15). These measurements were made at each load increment to establish the vertical profile of the loaded pier.

The lateral soil pressures mobilized in the front and back of the pier during each load increment were monitored by means of a number of earth pressure cells cast into the concrete pier such that they were in contact with the soil (Figure 16). The moment distribution along the length of the test footings was monitored by means of several welded strain gauges mounted on the rebars. Table II summarizes the types of instruments used in each test footing.

The details of the instrumentation of each footing are summarized in Appendix A..

TEST RESULTS

Table III summarizes the sequence of testing.

The recorded field data are summarized in Appendix B.

The load-deflection curves are shown in Figures 17 to 21. In the overturning moment tests, the moment to shear ratio could not be maintained constant throughout the test due to problems in the hydraulic pump system.

The rotation of the piers at different load levels, as determined by the slope indicator data, are shown in Figures 22 to 26. The lateral soil pressure distribution along the length of the footing, as measured by the earth pressure cells are shown in Figures 22 to 26. From the lateral pressure and footing deflection data the plots of p-y curves are constructed as shown in Figures 27 to 31.

ANALYSIS OF TEST DATA

From the collected test data the behaviour of the test footings was evaluated in terms of their load-deflection response and mobilization of

soil resistance against lateral loading. The measured data was compared with predictions made by a non-linear model called "PADLL" (Pier Analysis and Design for Lateral Loads).

Measured Load-Deflection Response

The load-deflection response was generally non-linear and the non-linearity increased with increasing stress level in the soil resisting the lateral loads. The creep movement measured over periods of 10 to 15 minutes also showed an increase with an increase in stress levels. The load tests were generally terminated when the ground line deflections approached 25 to 50 mm.

Test Footings 1 and 3 were loaded in uplift while Footing 2 was loaded in compression to their ultimate capacity before testing them under lateral loads. Footing 3 deflected more than Footing 2 which was of the same size as Footing 3, indicating some weakening in the lateral resistance due to the breakage of bond between the footing and the surrounding soil as a result of uplift loading prior to its lateral load test. Footing 1, with a diameter of 0.93 m and depth of 9.0 m, deflected more than Footings 2 and 3 which were of larger diameter but of shorter length such that the surface area of contact with the soil was the same.

In the working load range, the ground line deflections were inversely proportional to the diameter of the footings. Thus from considerations of lateral load behaviour of drilled piers in clay; a larger pole diameter will result in smaller line deflections.

Moment footings 6, 7 and 8 were loaded in pairs, initially with both top and bottom jacks to simulate the large moment to shear ratio of pole foundations. An average moment to shear ratio of 25 m was achieved in these tests. They were reloaded later with the top jacks only to induce large ground line deflections and to assess the ultimate load behaviour. Footings 6 and 7 were loaded close to their ultimate capacity, but Footing 8 with the largest diameter (2.76 m) and greatest depth (12.73 m), did not reach its lateral load capacity. Footing 8 deflected about 35 mm under the maximum applied moment of 2700 kN.m and a low moment to shear ratio of 2 m (Figure 21).

Prediction By Theoretical Model

The lateral load-deflection response of the test footings was predicted by using a computer code, PADLL (Pier Analysis and Design for Lateral Loads) which was developed by GAI Consultants for EPRI (Davidson 1982).

This computer code makes use of a theoretical model in which the applied shear and moment loads are resisted by the soil resistance on the sides and at the base of the pier as shown in Figure 32. The side resistance is modelled by one set of compression and shear springs, while the base resistance is modelled by another set of compression and shear springs. The governing equations for these springs are empirically derived by considering the deformation modulus of the soil and the geometry of the footing (depth to width ratio). The lateral compression spring is treated

as a non-linear spring while the other three springs are treated as linear elastic-plastic springs (Figure 32).

The soil deposit in which the pier was embedded is divided into a number of layers with their appropriate deformation modulus, shear strength and unit weight from which the spring constants are computed.

The deflections and rotation of the footing at various load levels are computed by solving the equilibrium equations in which the applied shear and moment forces are equated to the mobilized shear and moment of the four spring model. In this model the footing is assumed to rotate and translate as a rigid body.

The relationship between lateral pressure and lateral deflection is modelled by using p-y curves similar to those developed by Reese et al 1977. A schematic p-y curve is shown in Figure 32 in which the lateral pressure p, is shown to be non-linearly related to the lateral deflection, y. A secant to this curve corresponds to the horizontal subgrade modulus. The subgrade modulus is thus also non-linearly related to deflection.

The PADLL program uses the following equation to represent the p-y relationship:

$$p = 0.6\, p_{ult} \left(\frac{2k_h y}{p_{ult}}\right)^{0.5} \quad \text{.....(1)}$$

The subgrade modulus is given by:

$$k_h = 5.7\ E_s (D/B)^{-0.40} \quad \text{.....(2)}$$

where E_s = deformation modulus of soil
B = width of footing and
D = depth of footing

The ultimate soil resistance p_{ult} is given by Brinch Hansen's lateral bearing capacity formula:

$$p_{ult} = q\, k_q + c\, k_c \quad \text{.....(3)}$$

where q = surcharge pressure
c = cohesion strength
and k_c and k_q are lateral bearing capacity factors which are functions of the soil properties and the depth to width ratio.

According to this model (Equations 1 to 3)the lateral load-deflection response is influenced by not only the deformation modulus E_s, but also by the ultimate soil resistance, p_{ult} and the depth to width ratio of the footing.

Comparison Between Predicted and Measured Reponses of Test Footings

The lateral load behaviour of Footings 1, 2, 3, 6, 7 and 8 were analyzed by using the PADLL program. The soil deposit of 14 m thickness was divided into 7 layers with input soil parameters as shown in Table IV.

The top layer (layer 1) represented the gravel working pad placed before the start of construction. Its friction angle and deformation modulus were estimated to be 38 and 5 MPa respectively.

Layer #2 represented the silty sand layer of about 1.2 m thickness. Its lateral load behaviour under short term loading was modelled in two ways.

In Analysis #1 it was treated as a cohesive soil with an undrained shear strength of 75 kPa (estimated) and a deformation modulus of 30 MPa (from self boring pressuremeter test).

In Analysis #2 this silt layer was considered as a cohesionless soil with a friction angle of 31 and a deformation modulus of 30 MPa.

The Leda clay deposit extending beneath 1.5 m depth was divided into 5 layers and each layer was assigned an undrained shear strength value (as determined by piezocone and dilatometer tests) and an undrained modulus value (as determined by the reloading cycle of self boring pressuremeter tests).

Footings With No Overturning Moment

Figures 33 and 34 show the comparison between the predicted and measured load-deflection responses of Footings 1 and 2 and 3 for which only ground shear was applied with no overturning moment.

Since the PADLL program does not predict deflection due to creep during hold loads, the measured response curves used for comparison in Figures 33 and 34 are obtained by deducting the creep portion of deflection at each load increment.

The following observations are made from Figures 33 and 34.

1. The predicted load-deflection responses were similar for all Footings 1, 2 and 3 both in Analysis #1 or #2. However, the ultimate loads for Footing 1 (0.9 m diameter and 9.65 m deep) and Footing 2 or 3 (1.5 m diameter and 6.40 m deep) were significantly different, being 780 kN and 941 kN respectively (Tables V and VI).

2. The assumption regarding the strength behaviour of the 1.2 m thick silty sand layer at the top as a cohesive or cohesionless material made a substantial difference in the predicted responses of footings.

3. In the case of Footing 1, both Analysis #1 and #2 under predicted the ground line deflections by a factor of 2 to 3.

4. In the case of Footings 2 and 3, Analysis #1 under-estimated, while Analysis #2 over-estimated the deflections.

5. Comparing the load-deflection responses of Footings 2 and 3, which were identical in size, the larger deflections of Footing 3 are attributed to the fact that it was tested in uplift prior to lateral loading.

6. The lateral load-deflection response of Footings 1 and 3 was severely affected by their testing in uplift to failure prior to lateral loading. The loading in uplift to ultimate capacity has the effect of breaking the bond between the concrete and the clay at its sides and bottom.

7. Footing 1, which was only 0.9 m in diameter and 10 m in length, showed internal bending under the maximum applied load (Figure 22). The PADLL analysis does not account for the pier bending as it assumes the pier to be rigid.

For lattice type towers with pier foundations the design shear force per footing is in the range of 220 to 300 kN. From the results of tests on Footings 2 and 3, it is estimated that the lateral deflections of drilled pier foundations for lattice type towers in Leda clay deposit will not exceed 10 to 15 mm.

Moment Footings

Figures 35 to 42 show the comparison between the predicted and measured moment-deflection responses for test Footings 6, 7 and 8. Footings 6 and 7 were initially tested against Footing 8 (Tests 10 and 11). Then Footing 8 was loaded with Footing 6 as the reaction (Test 12). Each of these 3 footings were subjected to combined shear and moment loading. Initially they were tested under a moment to shear ratio or eccentricity of 23 to 25 m (Tests 10a and 11) then they were reloaded under a moment to shear ratio of 2 to 2.5 m (Tests 10b and 12). Table III summarizes the testing sequence adopted. From this sequence it can be inferred that Footing 8 (2.7 m diameter by 13 m deep) was loaded in one direction (Tests 10a and 10b) and then it was reloaded in the opposite direction (Tests 11 and 12).

For purposes of comparing with predicted deflections the measured load-deflection response curve is reconstructed by discounting the creep movements recorded for each load application. The load-deflection behaviour was predicted by using the PADLL program. The soil parameters were input in the same way as for Footings 1, 2 and 3 (Table IV). Two sets of input parameters were employed for the upper 1.2 m thick silt layer. Analysis 1 considered the silt layer to behave as a cohesive soil with an undrained shear strength of 75 kPa, while Analysis #2 considered the silt layer to behave as a cohesionless soil with a friction angle of 31°. In both cases the deformation moduli were identical and equal to the self boring pressuremeter values (Table IV). After examining Figures 35 to 42, the following observations can be made.

1. Analysis #1, in which the top silt layer is assumed to behave as a cohesive soil, gave a closer prediction of the ground line deflections than Analysis #2 in which the silt layer is assumed to behave as a cohesionless soil.

2. In the case of Footings 6 and 7 which were only 6.5 m deep, Analysis #2 overpredicted the deflections (Figures 35 and 36).

3. In the case of Footing 8 (2.8 m diameter by 13 m deep) the differences between the results of Analysis #1 and #2 are less pronounced compared to the case of Footings 6 and 7, suggesting that the significance of the surface layer behaviour (cohesive or cohesionless) diminishes with deeper footings (Figures 35 to 38).

4. In comparing the predictions with measured deflections of Footing 8 in Test 11 (Figure 38) a correction for the measured response curve was made to account for the effects of the reversal of loads between Tests 10b and 11. After applying this correction to the measured response, a good agreement with the prediction is obtained.

5. In general, the PADLL program (Analysis #1) modelled well the non-linear load-deflection response of the moment Footings 6, 7 and 8. The best match between the predicted and measured responses was obtained for Footing 7 (Test 10a) using Analysis #1 (Figure 35).

6. For the loading case with a small moment to shear ratio or an eccentricity of only 2 m as in the case of Footing 8 (Test 12), the PADLL program under-predicted the deflections (Figure 39).

7. The effect of varying the stiffness of Leda clay (indicated by its deformation modulus) on the deflection predictions is shown in Figures 40 to 42. By changing the deformation modulus of the clay from 12 MPa (self boring pressuremeter value) to 6 MPa (laboratory triaxial value), the predicted deflections increased marginally for Footing 7 (Figure 40) and by about 50 per cent for Footing 8 (Figure 41).

8. Non-recoverable deflections in the range of 30 to 50 per cent of total deflections were recorded under maximum applied loads. The PADLL program also predicted the non-recoverable deflection in the range of 50 per cent of total deflections (Table XII).

Footing Deflection and Soil Pressure Distribution

Figures 22 to 26 show the measured deflections and soil pressures along the embedded portion of the test footings. The footing deflections were obtained by either the slope indicator data or the tilt meter readings at the ground level. The soil pressures were recorded by pressure cells embedded in the sides of the footings.

The following observations can be made from this:

1. All footings except Footing 1 rotated as rigid piers without bending.

2. The centre of rotation was located at a depth of about one-half to two-thirds of the embedded length of each footing. The centre of rotation was generally deeper for Footings 1, 2 and 3 which were loaded with no overturning moment.

3. The recorded soil pressures were relatively small until the applied loads reached their maximum value. In the case of Footing 1, the recorded soil pressures were substantially smaller than anticipated. This may have been due to the fact that this footing was tested in uplift to failure before loading it in the lateral direction. Also, the Leda clay may tend to flow around the footing due to its soft consistency, especially in the case of Footing 1 with its small diameter.

4. The pressure cells located above the centre of rotation and in front of the footing recorded lower pressures than those located below the centre of rotation and behind the footing. This is probably due to the confinement effect from the overburden.

5. No pressure cells were located in the upper silt layer and therefore no data is available about its contribution to the lateral soil pressures.

Comparing the PADLL predicted deflections and the soil pressures from Analysis 1 with the measured data (Tables VII to X), the following observations can be made:

1. The predicted soil pressures were higher than those measured except in the case of Footing 8 (Tables XVI) which was loaded with a zero or small moment to shear ratio.

2. The predicted deflections were much smaller than those measured except for Footings 6, 7 and 8 which were loaded with high moment to shear ratios.

3. The predicted higher soil pressures and smaller deflection of footings in the embedded portion imply that the stiffness of the Leda clay used in the PADLL Analysis is higher than that indicated by direct measurements.

To examine the influence of the clay stiffness, predictions of Analysis #1 were repeated with the deformation modulus value obtained by the laboratory triaxial tests (an average value of 6 MPa) instead of the self boring pressuremeter modulus(an average value of 12 MPa). Comparing these predicted responses with the measured responses (Figures 40 to 42) it can be inferred that the deflection predictions are not significantly different in the working load range.

DESIGN CONSIDERATIONS

From the foregoing analysis of the full scale foundation test data and in

situ soil property measurements at the Gloucester site, the following general conclusions can be drawn:

1. The lateral load behaviour of drilled piers in soft clay can be significantly affected by the presence of a strong and stiff layer at the surface. This effect decreases with increasing embedment depth (or D/B ratio) and the moment to shear ratio (eccentricity) of loading.

2. The PADLL program (developed for EPRI) which is based on the four spring model, predicts well the non-linear behaviour of moment loaded drilled piers.

3. The PADLL prediction of load-deflection response for the test footings was sensitive to whether the surface silt layer was treated as a cohesive or as a cohesionless soil. The later assumption generally yielded larger deflections.

4. By treating the surface silt layer as a cohesive soil, with an undrained shear strength of 75 kPa, good agreement between the predicted and measured deflections was obtained for the case of moment footings (ie Analysis #1).

5. PADLL predictions were not good for footings which were subjected to a low moment to shear ratio. In its development, the PADLL program was calibrated with respect to full scale pole foundation test data performed at several sites in the United States (Davidson, 1982). In these tests a high moment to shear ratio was employed to simulate the steel pole loading. This calibration process may have adversely affected the ability of PADLL to predict behaviour of low moment to shear loaded footings.

6. Undrained shear strength values obtained by piezocone tests were in agreement with NGI vane results, while the laboratory triaxial and dilatometer values were on the low side.

7. The deformation modulus values of Leda clay obtained by the self boring pressuremeter test were twice the values obtained by the laboratory triaxial test on undisturbed samples.

8. In the working load range, the predicted deflection of full scale pole foundations is proportional to the deformation modulus of the clay deposit.

9. Except for Footing 8, all of the footings were loaded to their ultimate capacity. From a comparison between the predicted and measured ultimate capacities (Table XI), it is seen that Footings 1, 2 and 3 were weaker than predicted, while for the moment Footings 6 and 7, the predictions were close to the applied maximum loads.

10. Comparing the deflections measured and predicted under maximum applied loads, good agreement was obtained only for the moment Footings 6, 7 and 8 with large moment to shear ratio (Table XII).

In order to assess the design implications of the findings from this field test program and the analysis by the PADLL program, an example case of pole foundation design is worked out as follows:

Tower type: V2S single steel pole

Pole Height = 46 m

Foundation Loading: Groundline Shear = 222 kN
Groundline Moment = 12,690 kN.m
Moment/shear Ratio = 57 m

Pier Diameter = 2.4 m

Allowable Maximum Deflection at Groundline = 19 mm, 12 mm or 6 mm

Pier Embedment Length = ? (to be calculated)

Soil Parameters

Uniform Leda clay deposit with no sand or silt layer at the top

Undrained Shear Strength = 30 kPa (based on piezocone test data)

Deformation Modulus = 12 MPa (Based on self boring pressuremeter tests)

or 6 MPa (based on laboratory triaxial tests)

Table XIII summarizes the embedment depths calculated by the PADLL program for three sets of permissible maximum groundline deflections and two sets of deformation modulus values for Leda clay. From this table it can be seen that for a permissible groundline deflection of 19 mm, an embedment depth of 13 m is required if the self boring pressuremeter modulus of 12 MPa is used. The footing will be 2.4 meters deeper if the laboratory modulus value is used in the analysis. Similarly for lower tolerance limits on groundline deflection of 12 mm and 6 mm, the footing depth required increases by 1.3 m and 4.8 m respectively.

CONCLUSIONS

Augering holes with diameters of up to 2.7 m and depths of up to 13 m did not pose any caving problems. Dry augering with cleats welded on the flights retained the excavated clay successfully. Unless very bad caving conditions are anticipated, tremie construction methods should be avoided. Bentonite slurry should never be used. Augered holes to depths greater than 10 m should not be left open for more than 4 to 6 hours.

The load deformation behaviour of the laterally loaded piers in Leda clay is non-linear. The presence of the surface silty sand layer which was stronger and stiffer than Leda clay influenced the deflection behaviour of test footings, especially those that were loaded with no overturning moment.

The PADLL program, based on four spring model predicted the load-deflection response of moment footings fairly well. The predictions were not good for the footings which were tested under uplift and compression prior to lateral loading. The recorded soil pressures along the length of the test footings were generally smaller than PADLL predictions.

It is recommended that the deformation modulus values determined by the reload portion of the triaxial tests and the undrained shear strength values determined by piezocone or dilatometer can be used for the calculation of pier embedment depths for steel pole structures. This procedure will yield a somewhat greater footing depth than the one estimated on the basis of self boring pressuremeter modulus values. However, this margin of error on the safe side will allow for any additional deflections that may result due to the effects of repeated loading or reversal of loading.

The ultimate shear and moment capacities can be estimated from the PADLL program which are based on Brinch Hanson's earth pressure coefficient.

ACKNOWLEDGEMENTS

The successful completion of this field testing program is the result of a team effort and assistance provided by many departments of Ontario Hydro and outside agencies. The following are acknowledged for their valuable contributions:

1. The National Capital Commission and the Department of National Defense for permitting the field work to be carried out on their property at Gloucester Naval Base.

2. The National Research Council for their technical cooperation in performing in situ soil property measurements and instrumentation of the test footings.

3. The Electric Power Research Institute for allowing us to use the PADLL program in the analysis of the test data.

4. Mr. D. Fraser, Mr. M. Grills and Mr. P. Adams for carrying out installation and monitoring of the instruments.

5. The Mechanical Testing Section of the Mechanical Research Department for the load testing.

6. The Lines and Stations Construction Department in Ontario Hydro for installing footings and assistance in load testing.

Approved by:

T.W. Klym
Manager
Civil Research Department

Prepared by:

H.S. Radhakrishna
Senior Engineer
Soil Sciences Section

R. Tsang
Engineer
Soil Sciences Section

Reviewed by:

T.J. Carmichael
Supervising Engineer
Soil Sciences Section

HSR/RT:LM

REFERENCES

1. Crawford, C.B. "Quick Clays of Eastern Canada". Eng Geol 2:4, 239-265. 1968.

2. Crawford, C.B. and W.J. Eden. "A Comparison of Laboratory Results with In situ Properties of Leda Clay". Proc 6th Int Conf Soil Mech Found Eng, (1), 32-35, Montreal. 1965.

3. Law, K.T., M. Bozozuk and W.J. Eden. "Measured Strengths Underfills on Sensitive Clays". Proc 9th Int Conf Soil Mech Found Eng (1) 187-192. (1977.

4. Davidson, H.L. "Laterally Loaded Drilled Pier Research". Vol 2 EPRI Report EL-2197. 1982.

5. Bechai, M. "In Situ Testing Methods and Their Application to Geotechnical Investigation for Transmission Lines". Ontario Hydro Research Division Report No 86-134-K. 1986.

6. Di Bagio, E. Private communications. NGI, Norway. 1985.

7. Cragg, C.B.H. and H.S. Radhakrishna. "Uplift and Compression Behaviour of Drilled Piers in Leda Clay". Ontario Hydro Research Division Report No 86-165-K. 1986.

8. Reese, L.C., and J.D. Allen. "Drilled Shaft Manual, Vol 11 - Structural Analysis and Design for Lateral Loading". US Dept Transportation, July 1977.

TABLE I

Summary of Footing Dimensions as Constructed

Footing Number	Steel Liner: Embedded Length (m)	Steel Liner: Projection Above Gravel Fill (m)	Footing Diameter: Cased Portion (m)	Footing Diameter: Uncased(i) Augered Portion (m)	Measured Augered Length (m)	Projection of Footing Above Gravel Fill (m)	Type of Load Tests
1+	2.59	0.76	0.94	0.91	9.65	0.30	uplift
2	1.83	0.30	1.55	1.45	6.40	0.46	compression
3	1.98	0.15	1.55	1.45	6.40	0.30	uplift
4+,*	1.45	0.69	1.55	1.45	6.81	0.30	uplift
5+,*	1.52	0.61	1.55	1.45	6.32	0.30	uplift
6	2.92	1.35	2.53	2.44	6.63	3.35	moment
7	3.20	1.37	1.70	1.50	6.93	3.33	moment
8:,*	2.79	1.47	2.79	2.72	12.73	3.35	moment
9	4.04	0.53	1.70	1.50	6.88	0.61	uplift
10	3.96	0.61	1.70	1.50	6.71	0.61	uplift
11	3.71	0.86	1.70	1.50	6.65	0.61	uplift

Additional Notes: All of the footings constructed in the dry with exceptions as noted:
(+) noticed soil disturbance at bottom of augered hole
(*) water added to support hole (4.27 m deep)
(:) minor caving at side of hole below liner after 5 hours being left open and reinforcing cage sank to depth of 12.95 m
(i) auger diameter plus estimated "auger whip" of 2.5 to 5 cm

TABLE II

Foundation Instrumentation*

A IN FOOTING

Footing No	Instrumentation Cast in Footing						
	Access Tubes	Base Piezometer	Strain Gauges	Load Cell	Pressure Cells Side	Pressure Cells Base	Inclinometer
1	1	✓	8	✓	4	-	✓
2	2	✓	6	✓	-	3	✓
3	1	✓	-	-	4	-	✓
4	2	✓	-	-	-	-	-
5	2	✓	-	-	-	-	-
6	1		-	-	6	-	✓
7	1		12	-	6	-	✓
8	1		-	-	6	-	✓

B BESIDE FOOTING

Footing No	Instruments in Soil			
	Piezometers (including base)	Settlement Gauges	Pressure Cells	Inclinometers
1	4	6	1	1
2	1	6	5	1
3	1	-	-	2

*see Appendix A for detailed location drawings of these instruments

TABLE III

Foundation Testing Sequence

Test Number	Test Footing(s)	Reaction Footing(s)	Test Type	Test Details	Test Footing Age (weeks)
6	2	3	shear	previously tested compression	12
	3	2	shear	previously tested uplift and shear	12
8	1	2	shear	previously tested uplift	13
	2	1	shear	previously tested (see above)	13
10a	7	8	moment & shear	scale (diameter) effect	6
10b	7	8	moment	previously tested (above)	6
11	6	8	moment & shear*	scale (diameter) effect	6
12	8	6,9,10 & 11	moment & shear**	scale (diameter) effect	6

* high moment to shear ratio (~25:1)
**low moment to shear ratio (~2:1)

TABLE IV

Summary of Soil Profile Used in PADLL Predictions

Soil Parameters: Number of Layers = 7 Depth to Water Table = 0.0 m

Layer Number	Depth to Bottom of Layer (m)	Total Unit Weight (kg/cu m)	Pressuremeter Modulus of Deformation (MPa)	Friction Angle (Degree)	Cohesion (kPa)	Strength Reduction Factor
1	0.3	1800	5	38	0	0.94
2	1.5	1800	30	0	75	1.00
3	3.0	1670	9	0	35	0.99
4	5.0	1600	11	0	25	0.99
5	7.0	1600	10	0	35	0.99
6	10.0	1600	13	0	30	0.94
7	14.0	1600	15	0	38	0.94

Layer #1 gravel fill $\emptyset = 38^{\circ}$

Layer #2 silty sand Cu = 75 kPa } Analysis #1

Layers 3 to 7 Cu for Leda clay based on Vesic's model

Soil Parameters: Number of Layers = 7 Depth to Water Table = 0.0 m

Layer Number	Depth to Bottom of Layer (m)	Total Unit Weight (kg/cu m)	Pressuremeter Modulus of Deformation (MPa)	Friction Angle (Degree)	Cohesion (kPa)	Strength Reduction Factor
1	0.3	1800	5	38.0	0	0.94
2	1.5	1800	30	31.0	0	1.00
3	3.0	1670	9	0.0	35	0.99
4	5.0	1600	11	0.0	25	0.99
5	7.0	1600	10	0.0	35	0.99
6	10.0	1600	13	0.0	30	0.94
7	14.0	1600	15	0.0	38	0.94

Layer #1 gravel fill $\emptyset = 38^{\circ}$

Layer #2 silty sand $\emptyset = 31^{\circ}$ } Analysis #2

Layer #3 Cu for Leda clay based on Vesic's model

TABLE V

Lateral Load Test on Footing #1

Diameter 0.93 m Embedded Length 9.65

for 80% of maximum lateral load (ie 335 kN applied)

Depth (m)	Lateral Pressure Distribution (kPa)		Deflection from Vertical (mm)	
	Measured	PADLL	Measured	PADLL
0	N/A	11	28 (24)	2.5
1.7	defective cell	140	16 (15)	1.8
4.8	7	45	3 (3)	0.6
6*	0	25	0 (0)	0.1
7.0	-10	-35	-4 (-4)	-0.2
9.0	-26	-75	-11 (-11)	-1

( ) footing deflections without creep
* estimated centre of rotation based on measured data

TABLE VI

Lateral Load Test on Footing #3

Diameter 1.50 m Embedded Length 6.40

for maximum lateral load (ie 505 kN applied)

Depth (m)	Lateral Pressure Distribution (kPa)		Deflection from Vertical (mm)	
	Measured	PADLL	Measured	PADLL
0	N/A	10	62 (28)	4.1
1.75	63	165	38 (17)	2.5
3.50	75	50	14 (6)	1.0
4.50*	0	7	0 (0)	0.1
4.70*	0	-5	-4 (-3)	-0.1
5.60	-115	-55	-17 (-7)	-0.9

( ) footing deflections without creep
* estimated centre of rotation based on measured data

TABLE VII

Overturning Moment Test on Footing #7

Diameter 1.6 m Embedded Length 6.9 m

for 76% of maximum shear load (ie 285 kN applied with eccentricity, e = 10.2 m)

Depth (m)	Lateral Pressure Distribution (kPa)		Deflection from Vertical (mm)	
	Measured	PADLL	Measured	PADLL
0	N/A	10	25 (17.5)	19
2.3	75	130	5 (8)	7.5
3.9	38	10	2 (1)	0
4.4*	0	-75	0 (-2)	-2
5.3	-53	-140	-5 (-7)	-7
6.4	-106	-200	-14 (-10)	-12

( )footing deflections without creep
* centre of rotation based on measured data

TABLE VIII

Overturning Moment Test on Footing #6

Diameter 2.5 m Embedded Length 6.6 m

for 86% of maximum shear load (ie 155 kN applied with eccentricity, e = 31.6 m)

Depth (m)	Lateral Pressure Distribution (kPa)		Deflection from Vertical (mm)	
	Measured	PADLL	Measured	PADLL
0	N/A	10	10	16
2.1	30	105	3	6
2.75 to 3.25*	0	50	0	2
3.5	-2	-10	-1	-0.5
4.5	-14	-90	-5	-5
5.8	-30 to -35	-160	-9	-11
6.3	-100 to -113	-180	-10	-13.5

*estimated centre of rotation based on measured data
no holds during testing

TABLE IX

Overturning Moment Tests on Reaction Footing #8

Diameter 2.8 m Embedded Length 12.7 m

for maximum shear load (ie 180 kN applied with eccentricity, e = 24.7 m)

Depth (m)	Lateral Pressure Distribution (kPa)		Deflection from Vertical (mm)	
	Measured	PADLL	Measured	PADLL
0	N/A	20	6	2.1
2.5	42	40	4	1.4
4.9	3	30	2	0.7
7.5 to 8.5*	0	0 to -25	0	0 to -0.3
8.8	-1	-25	-1	-0.3
10.9	-2	-50	-2	-0.9
12.6	-17	-65	-3	-1.5

*estimated centre of rotation based on measured data

NOTE: measured lateral pressure at a depth of 7.6 m was inconsistent with other pressure cells monitored

no holds during testing

TABLE X

Overturning Moment Test on Footing #8 (Test #12)

Diameter 2.8 m Embedded Length 12.7 m

maximum shear load (ie 1220 kN applied with eccentricity, e = 2 m)

Depth (m)	Lateral Pressure Distribution (kPa)		Deflection from Vertical (mm)	
	Measured	PADLL	Measured	PADLL
0	N/A	10.8	36	8.1
2.6	212	76	25	5.5
4.9	25	66	11	3.7
6 to 7*	0	67 to 55	0	2.7 to 1.8
7.6	0	46	5	0.5
10.9	70	-73	18	-1.5
12.6	112	-102	27	-3.3

*estimated centre of rotation based on measured data

No holds during testing

TABLE XI

Comparison Between the Predicted Ultimate Capacity and Applied Maximum Loads for Laterally Loaded Test Footings

Footing No	Predicted Ultimate Capacity*			Applied Maximum Loading		
	Shear (kN)	Moment (kN.m)	Moment to Shear Ratio (m)	Shear (kN)	Moment (kN.m)	Moment to Shear Ratio (m)
1	780	0	0	425	0	0
2	940	0	0	580	0	0
3	940	0	0	580	0	0
6	188	5,568	29.6	180	5,330	29.6
7	367	3,099	8.4	375	3,175	8.5
8 (Test #11)	643	19,053	29.6	180	5,330	29.6
8 (Test #12)	2,203	5,356	2.4	1,220	2,965	2.4

*for Analysis 1

TABLE XII

Comparison of Measured and Predicted Groundline Deflections Under the Maximum Applied Loads for Laterally Loaded Test Footings

Footing No	Total Groundline Deflections Near Maximum Applied Loading* (mm)		Non-recoverable Groundline Deflections (mm)	
	Measured	Predicted**	Measured	Predicted**
1	27	3	-	1.5
2	12	4	0.6	1.9
3	21	4	13	1.9
6	26	-	-	N/A
7	17.5	19	6.4	13
8 (Test #11)	5	2	-	0.9
8 (Test #12)	38	8	23.9	3.9

* Deflections without creep
**Analysis 1

TABLE XIII

Estimated Embedment Depths Required for
a Typical Pole Foundation from PADLL Program

Pier Diameter (m)	Groundline Tolerance (mm)	Average Soil Modulus, E (MPa)	Pier Embedment* Length Required (m)	Embedment Ratio D/B
2.4	19	12**	13.0	5.4
2.4	19	6***	15.4	6.4
2.4	12	12**	14.3	5.9
2.4	6	12**	17.8	7.4

* for V2S tower loading (shear = 222 kN, moment = 12,760 kN•m)
** based on self-boring pressuremeter tests at Gloucester test site
*** based on laboratory triaxial tests on samples from Gloucester test site

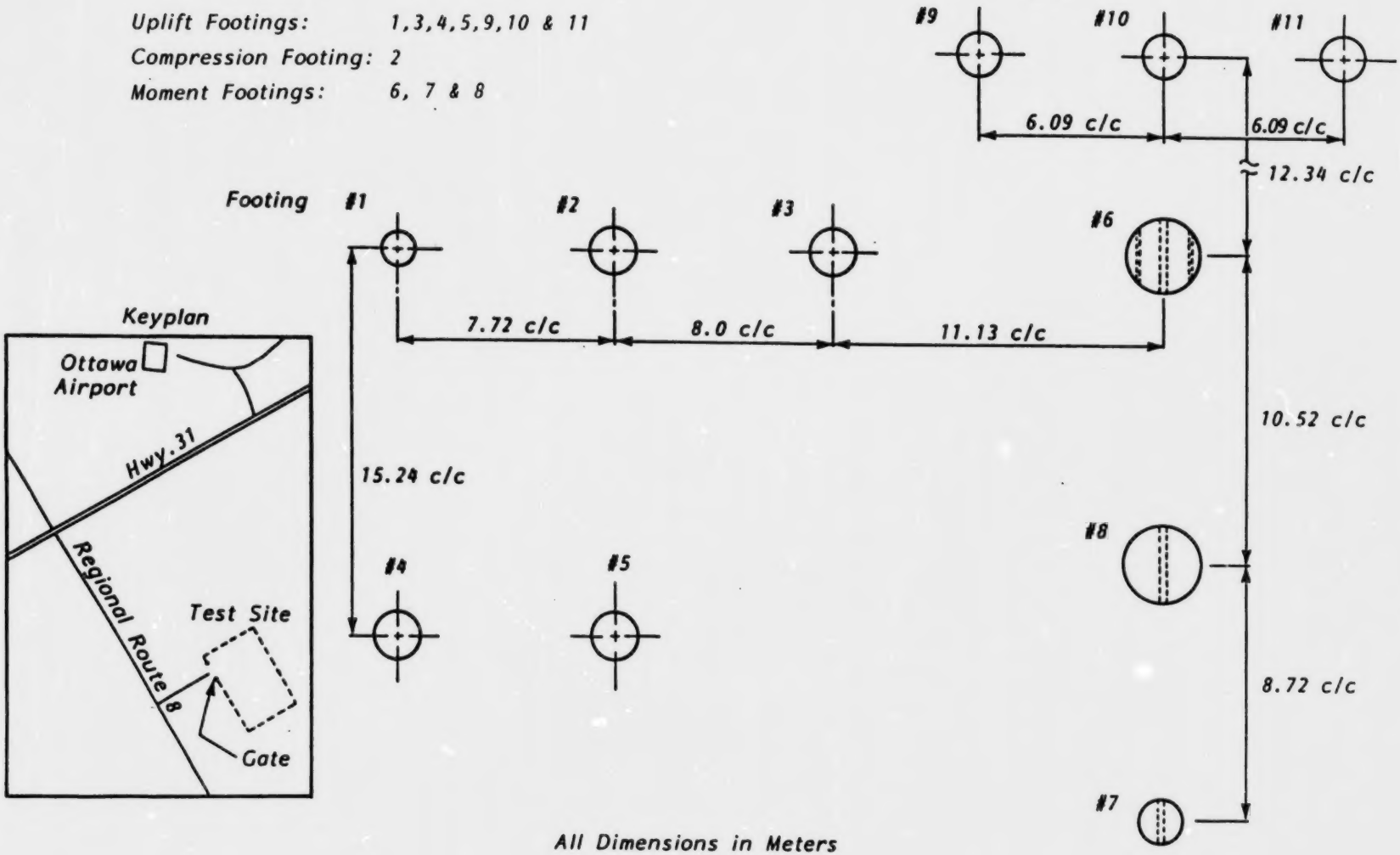

FIGURE 1

LAYOUT OF FOUNDATION FOOTINGS
AT GLOUCESTER TEST SITE

87-19

170516 RD

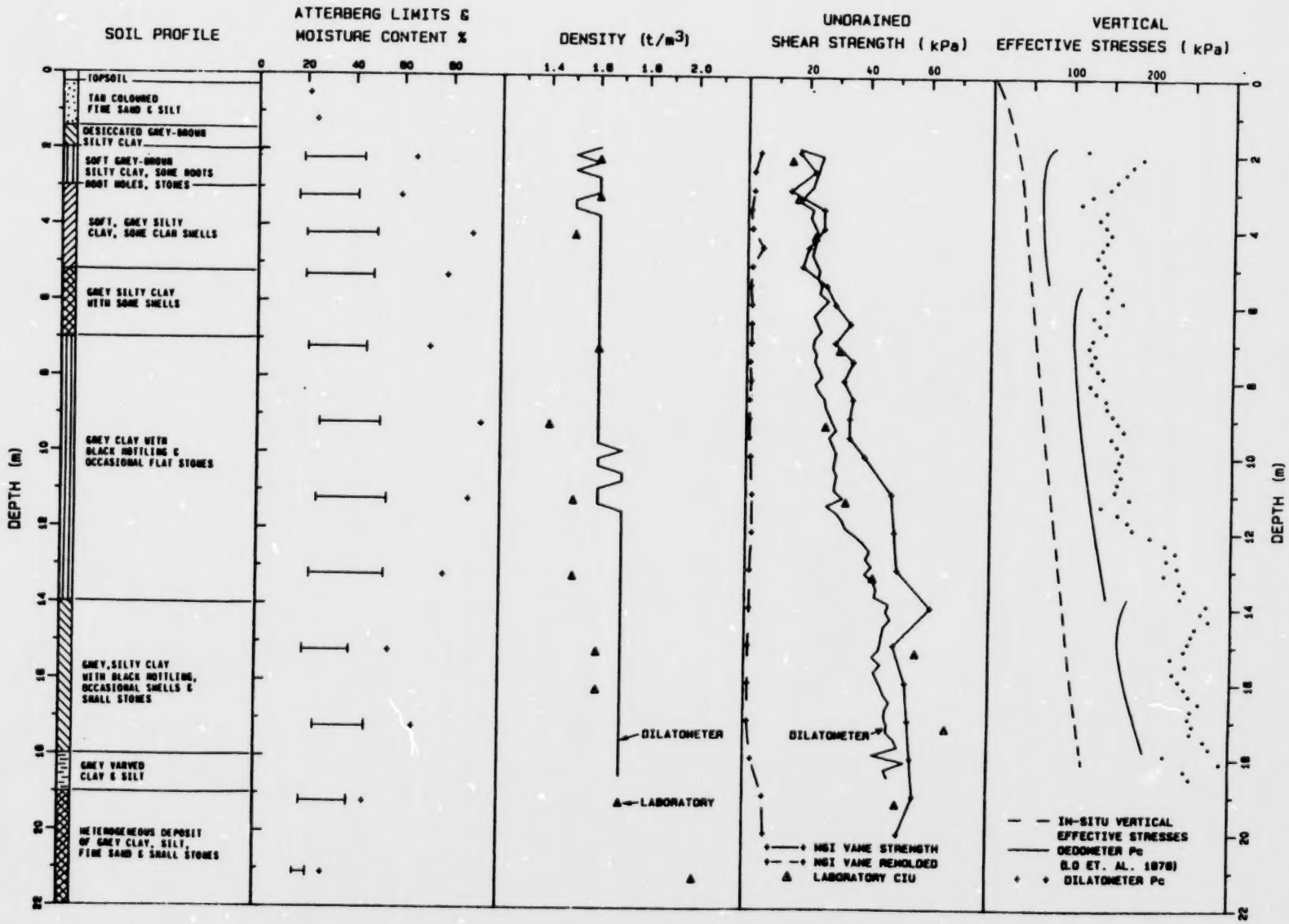
SOIL PROFILE
ATTERBERG LIMITS & MOISTURE CONTENT %
DENSITY (t/m3)
UNDRAINED SHEAR STRENGTH (kPa)
VERTICAL EFFECTIVE STRESSES (kPa)
DEPTH (m)
TOPSOIL
TAN COLOURED FINE SAND & SILT
DESICCATED GREY-BROWN SILTY CLAY
SOFT GREY-BROWN SILTY CLAY, SOME ROOTS ROOT HOLES, STONES
SOFT, GREY SILTY CLAY, SOME CLAM SHELLS
GREY SILTY CLAY WITH SOME SHELLS
GREY CLAY WITH BLACK MOTTLING & OCCASIONAL FLAT STONES
GREY, SILTY CLAY WITH BLACK MOTTLING, OCCASIONAL SHELLS & SMALL STONES
GREY VARVED CLAY & SILT
HETEROGENEOUS DEPOSIT OF GREY CLAY, SILT, FINE SAND & SMALL STONES
DILATOMETER
LABORATORY
DILATOMETER
NGI VANE STRENGTH
NGI VANE REMOLDED
LABORATORY CIU
IN-SITU VERTICAL EFFECTIVE STRESSES
OEDOMETER Pc (LO ET. AL. 1978)
DILATOMETER Pc

FIGURE 2

SOIL PROFILE FOR TEST SITE AT GLOUCESTER

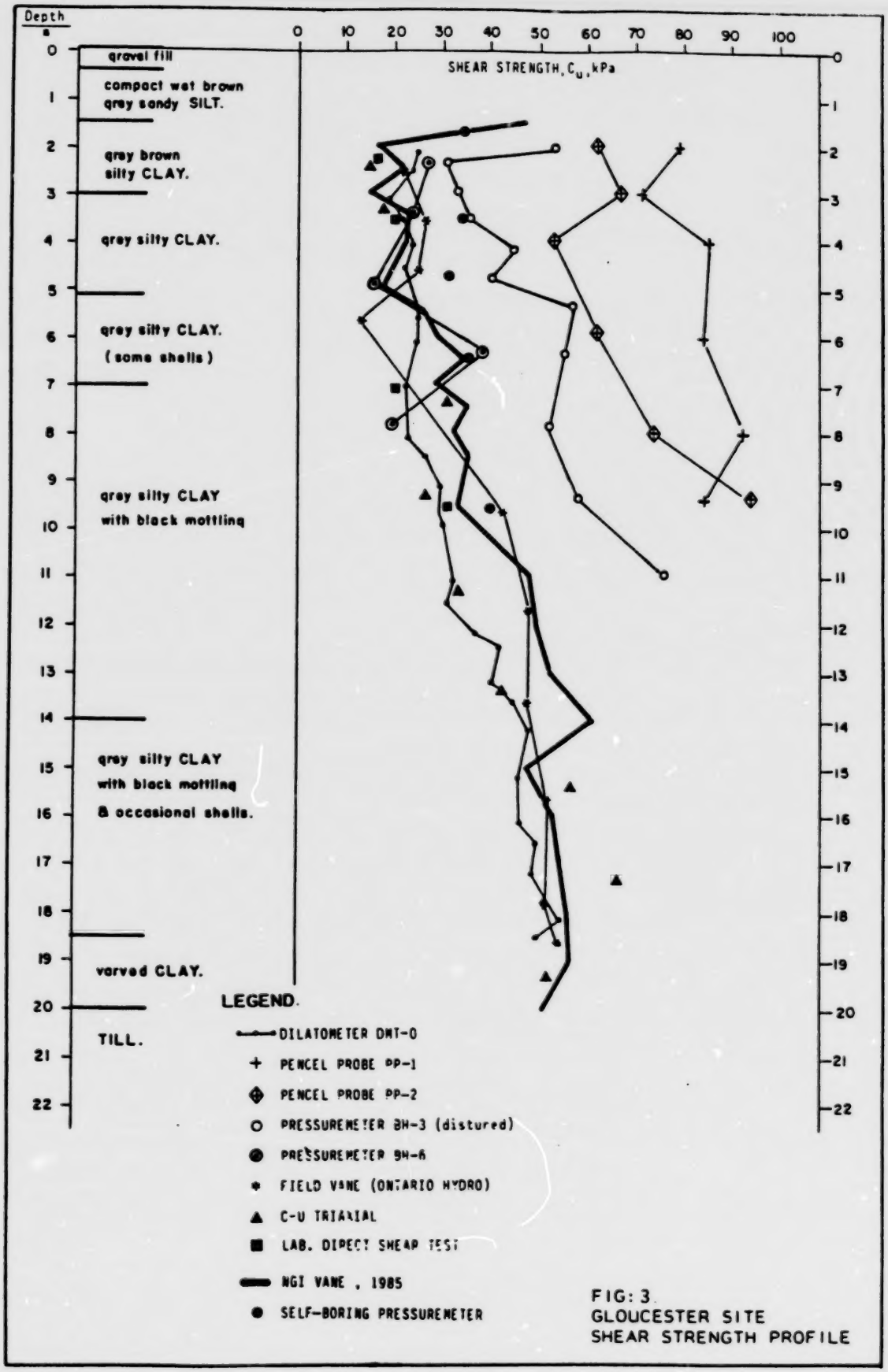

FIG: 3
GLOUCESTER SITE
SHEAR STRENGTH PROFILE

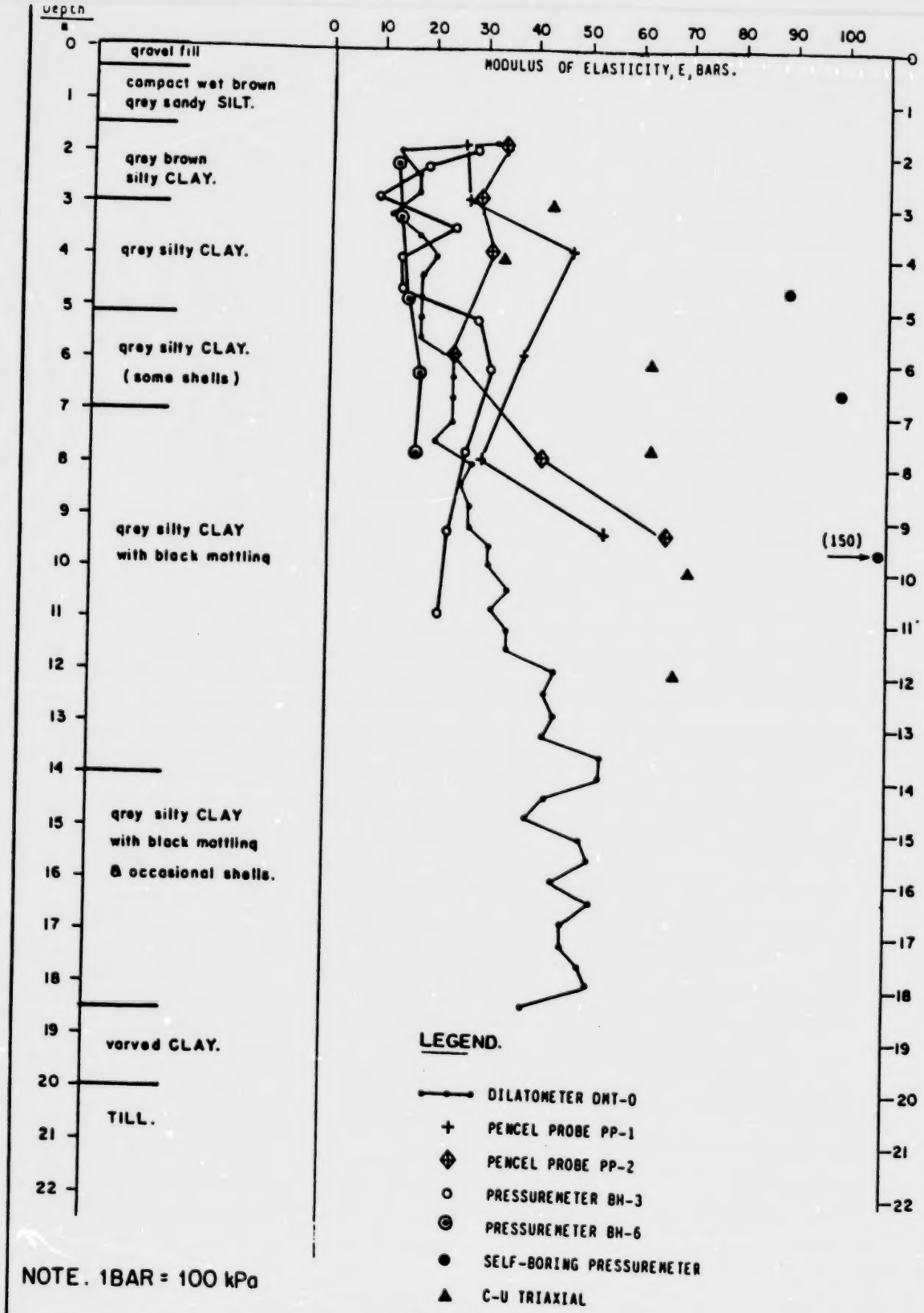

FIGURE 4
GLOUCESTER SITE
ELASTIC MODULUS PROFILE

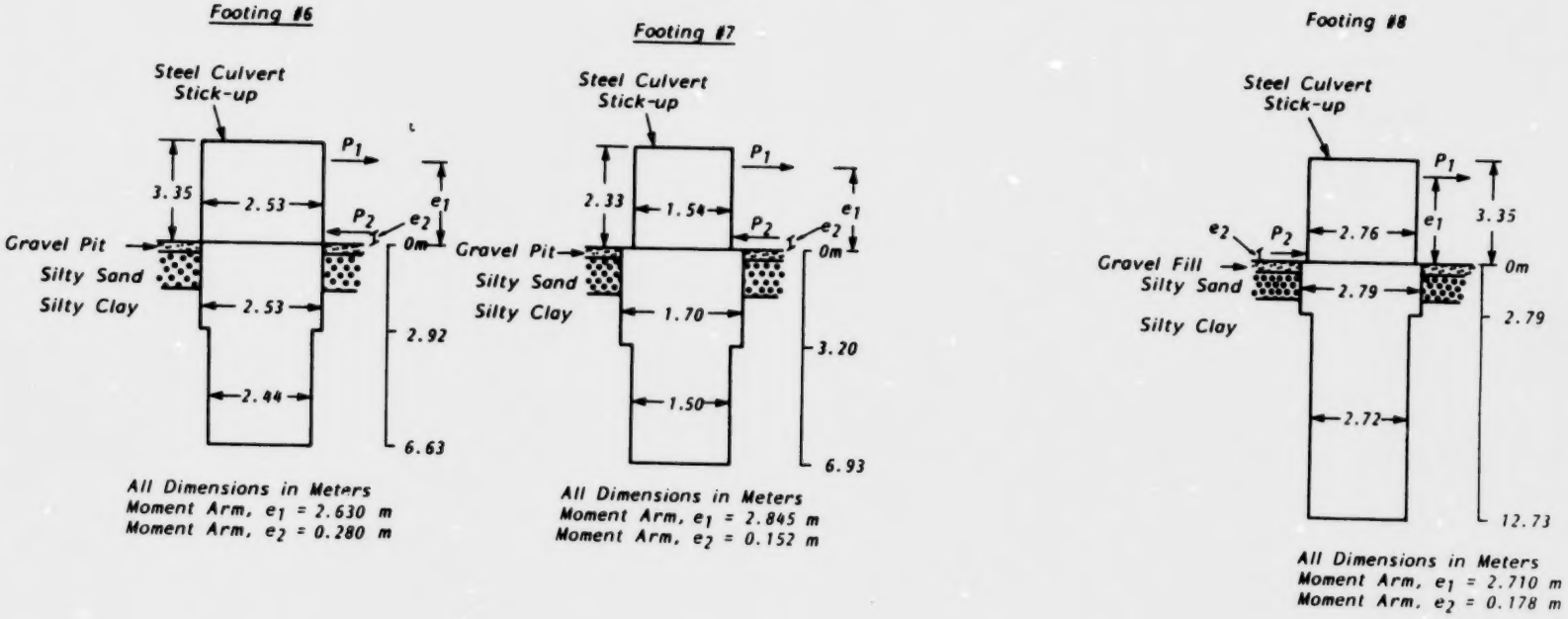

FIGURE 5

DIMENSIONS OF MOMENT FOOTINGS AS CONSTRUCTED

FIGURE 6

CLEATS WELDED ON THE AUGER FLIGHTS TO STOP THE EXCAVATED CLAY FROM SLIDING BACK INTO THE AUGER HOLE

FIGURE 7
AUGER TEETH MARKS AT THE BOTTOM OF HOLE

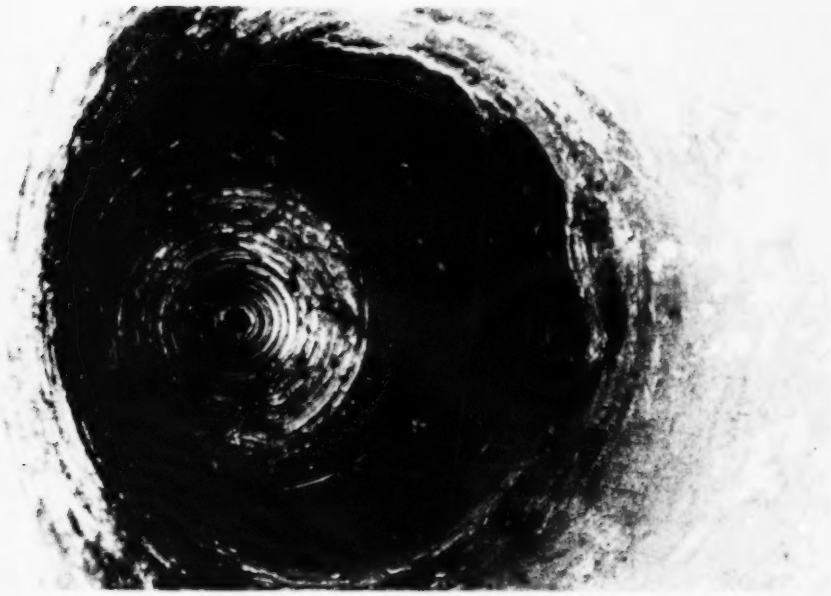

FIGURE 8
REMOULDED CLAY SMEAR ON THE SIDES OF HOLE

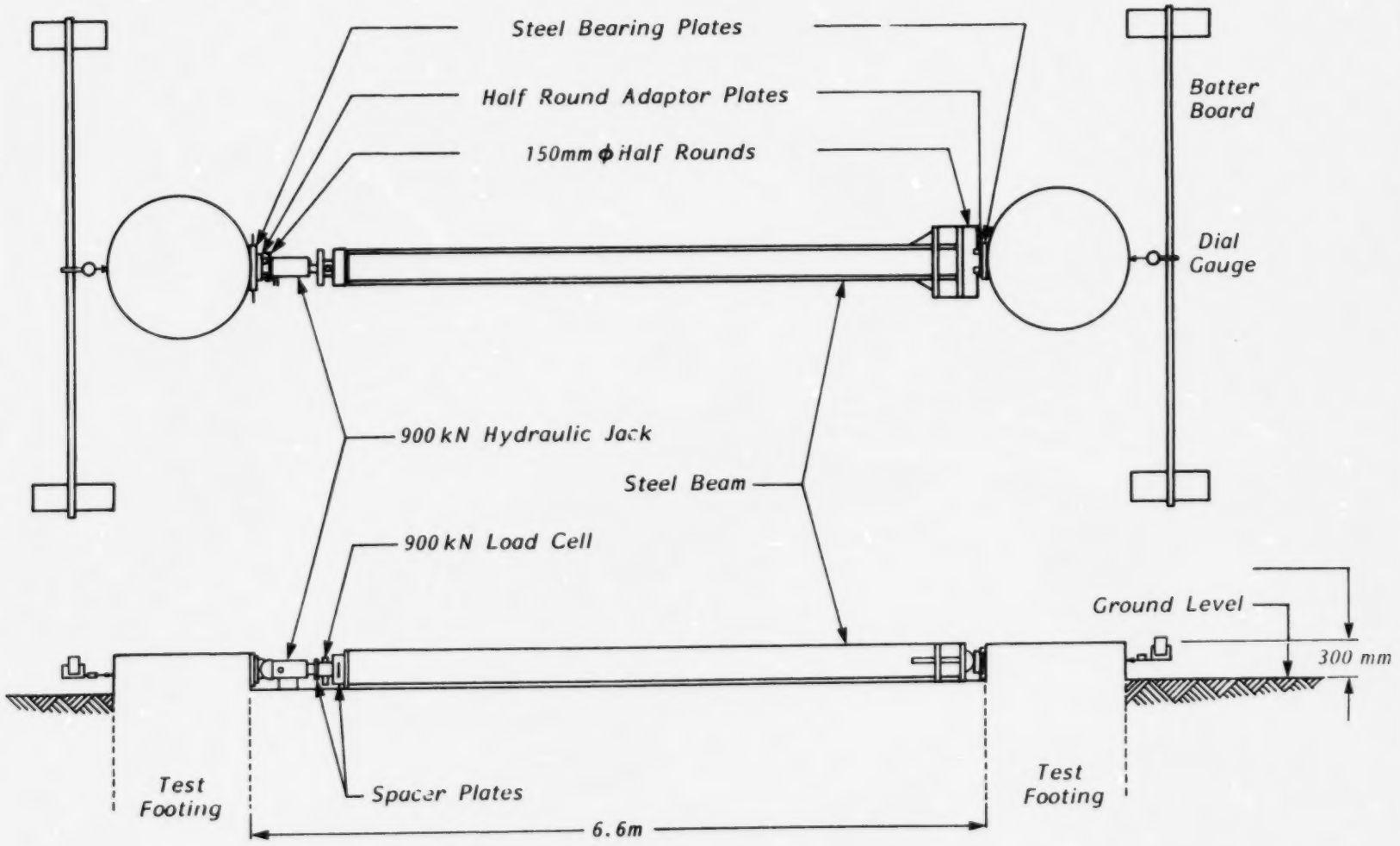

FIGURE 9
LATERAL LOAD TEST ARRANGEMENT

FIGURE 10
LOADING ARRANGEMENTS FOR FOOTINGS 1;2 AND 3

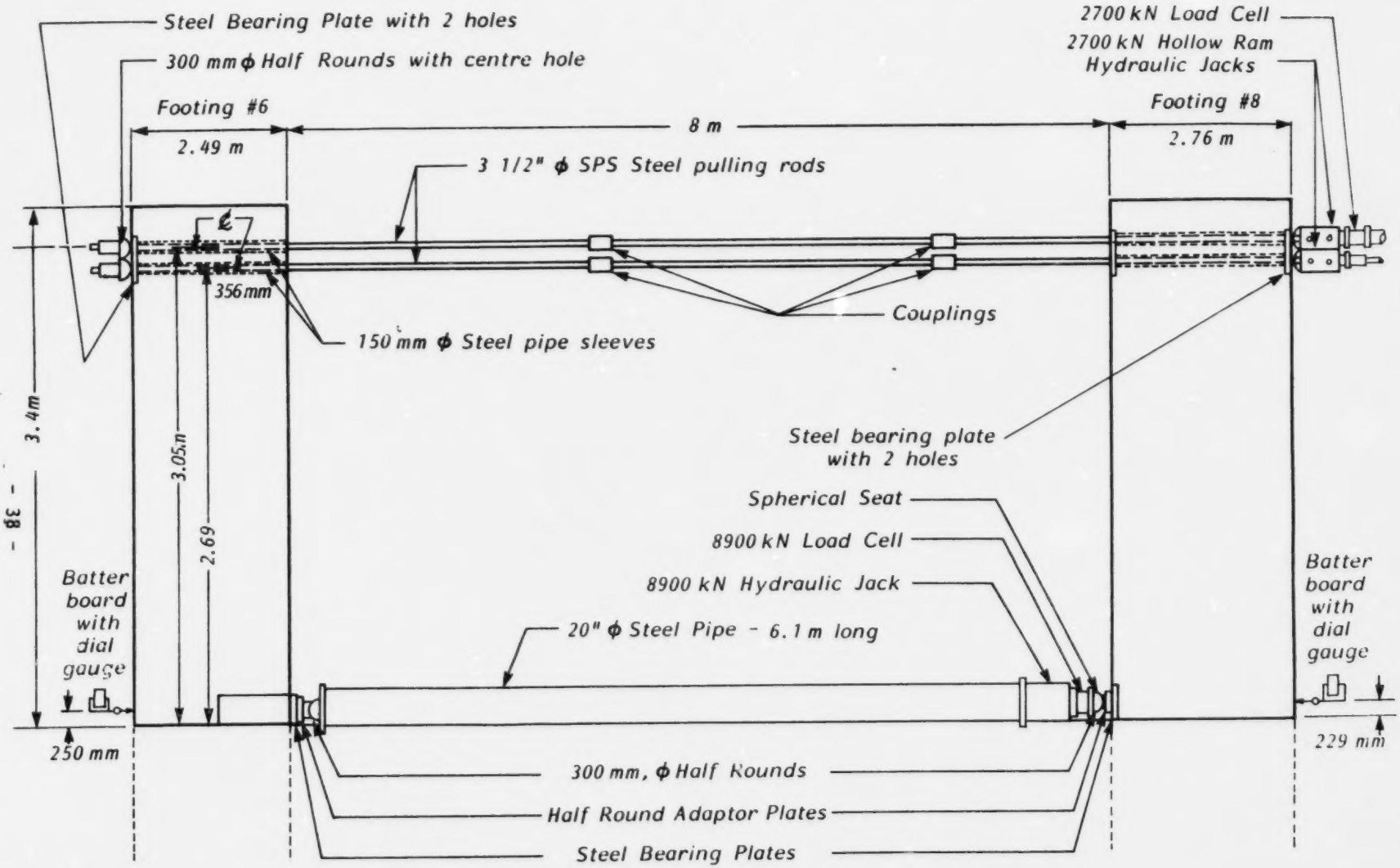

FIGURE 11

OVERTURNING MOMENT TEST ARRANGEMENT (TEST NO. 11)

87-19

170529 RD

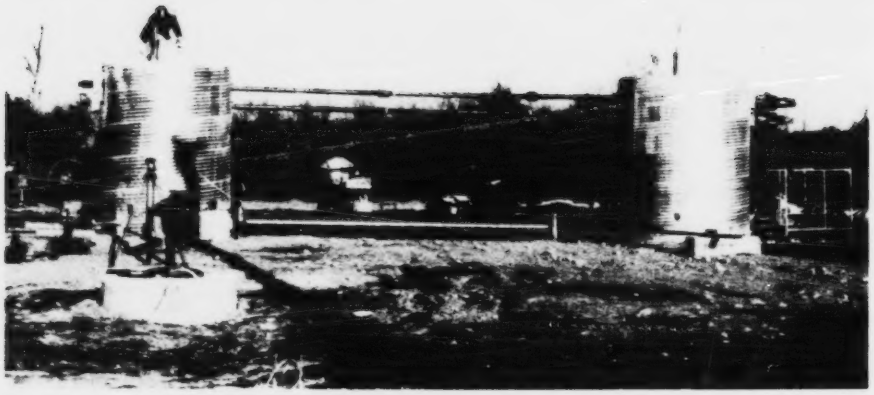

FIGURE 12
LOADING ARRANGEMENT FOR MOMENT FOOTINGS 6 AND 8

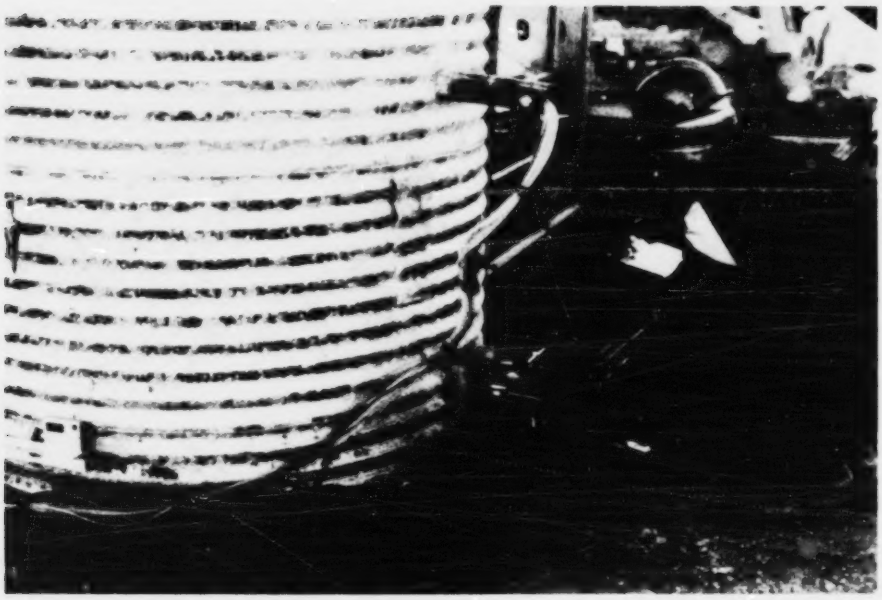

FIGURE 13

DIAL GAUGES AND LVDT FOR RECORDING
THE GROUND LINE DEFLECTIONS OF
MOMENT FOOTINGS

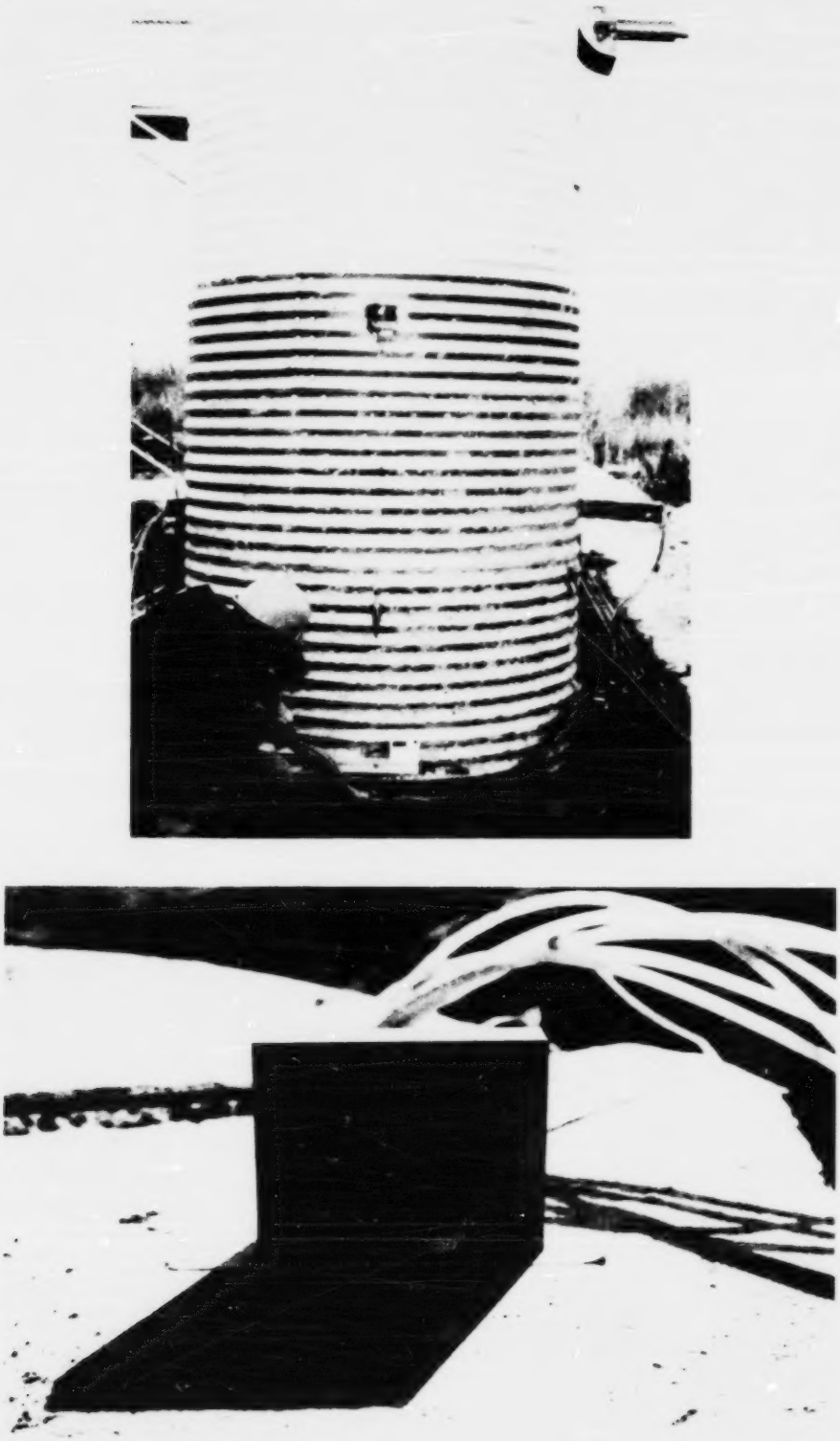

FIGURE 14

TILT METER TO RECORD THE
GROUND LINE ROTATION OF FOOTINGS

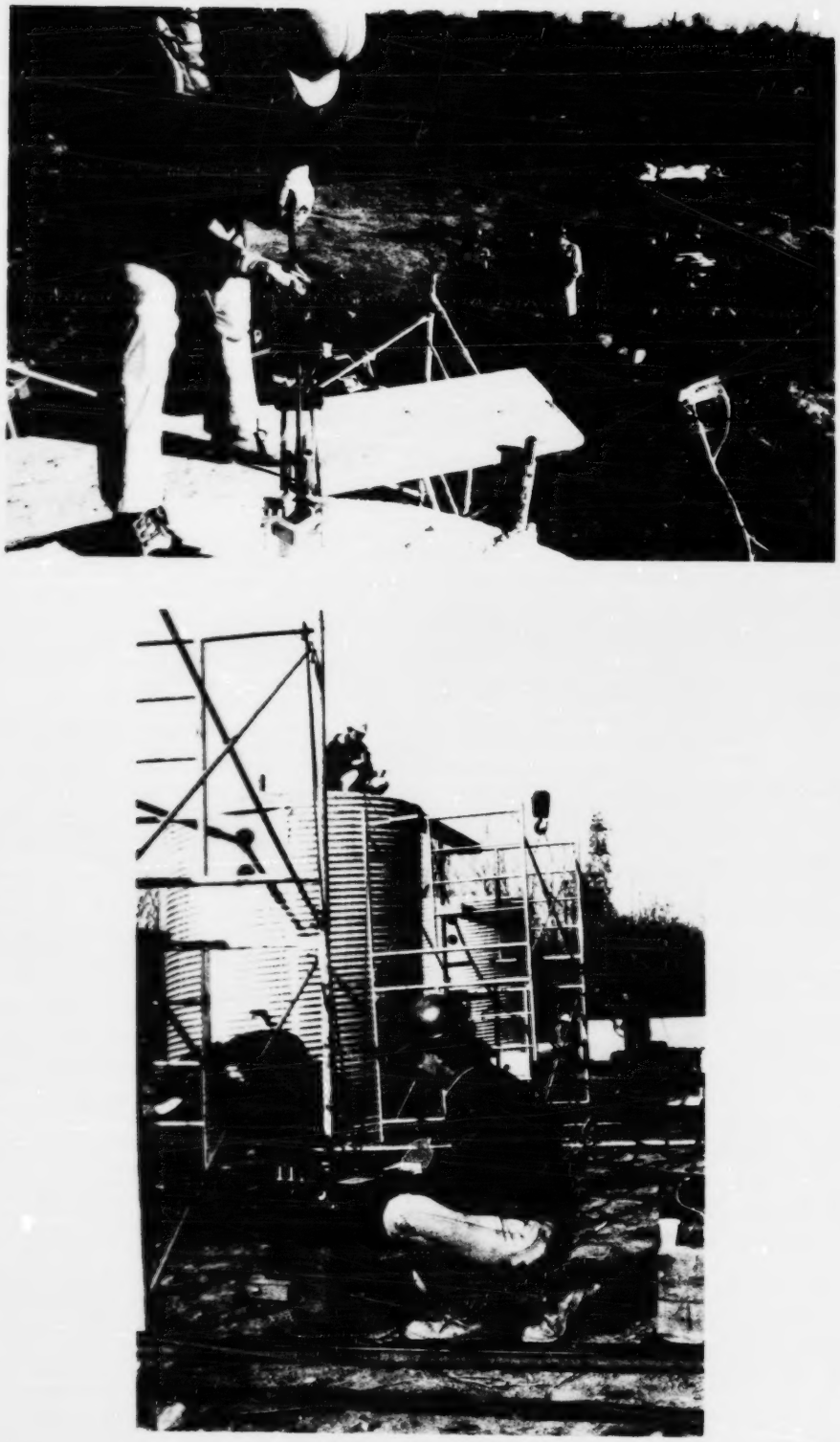

FIGURE 15
MEASUREMENT OF THE DEFLECTED FOOTING PROFILE
USING THE SLOPE INDICATOR

Cell Mounted On Re Bar Cage

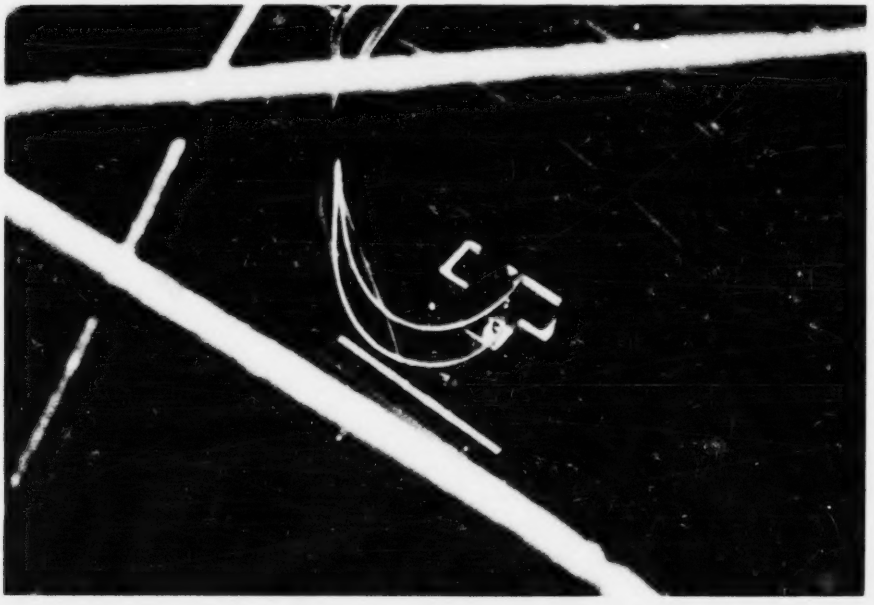

Pressure Cell In Contact With The Clay

FIGURE 16

EARTH PRESSURE CELLS MOUNTED ON STEEL REINFORCEMENT CAGE

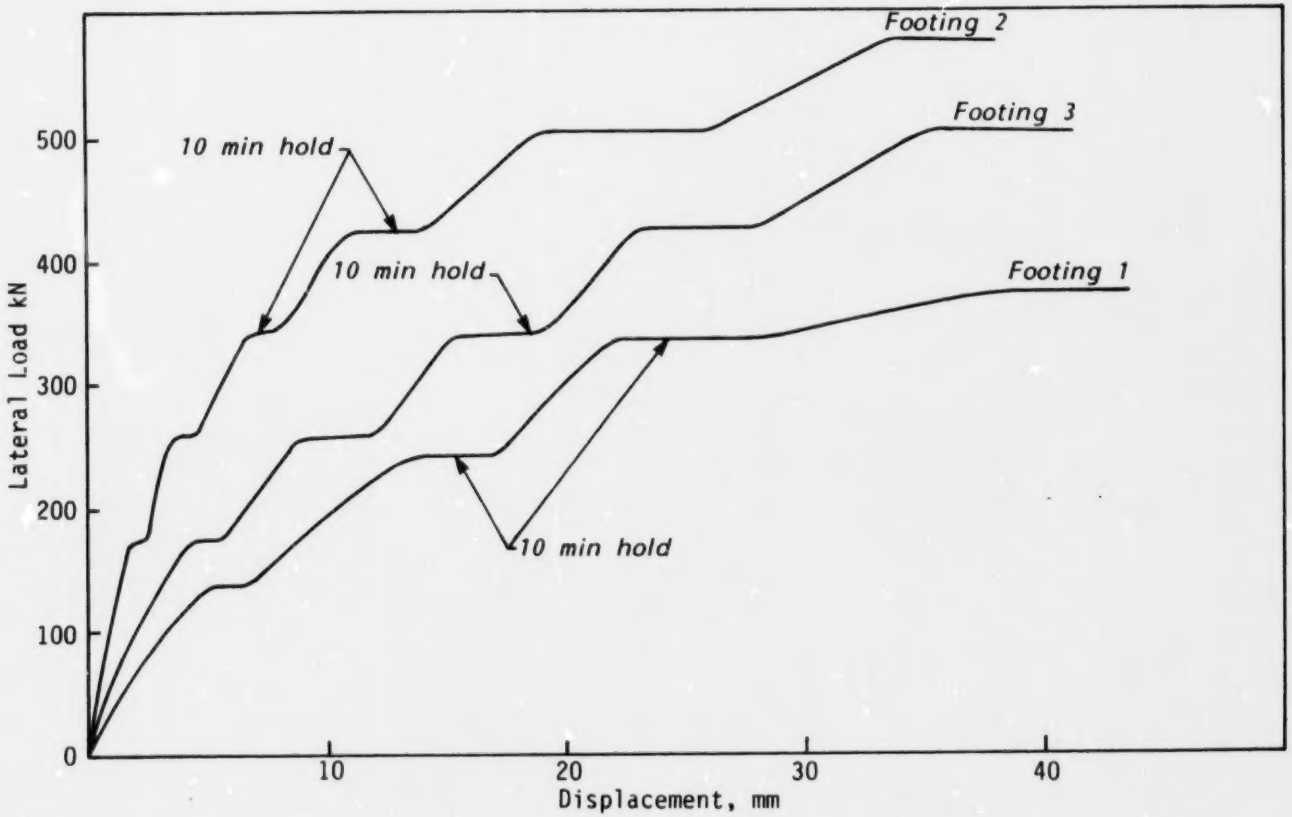

FIGURE 17
LATERAL LOAD DISPLACEMENT RESPONSE OF FOOTINGS 1, 2 AND 3

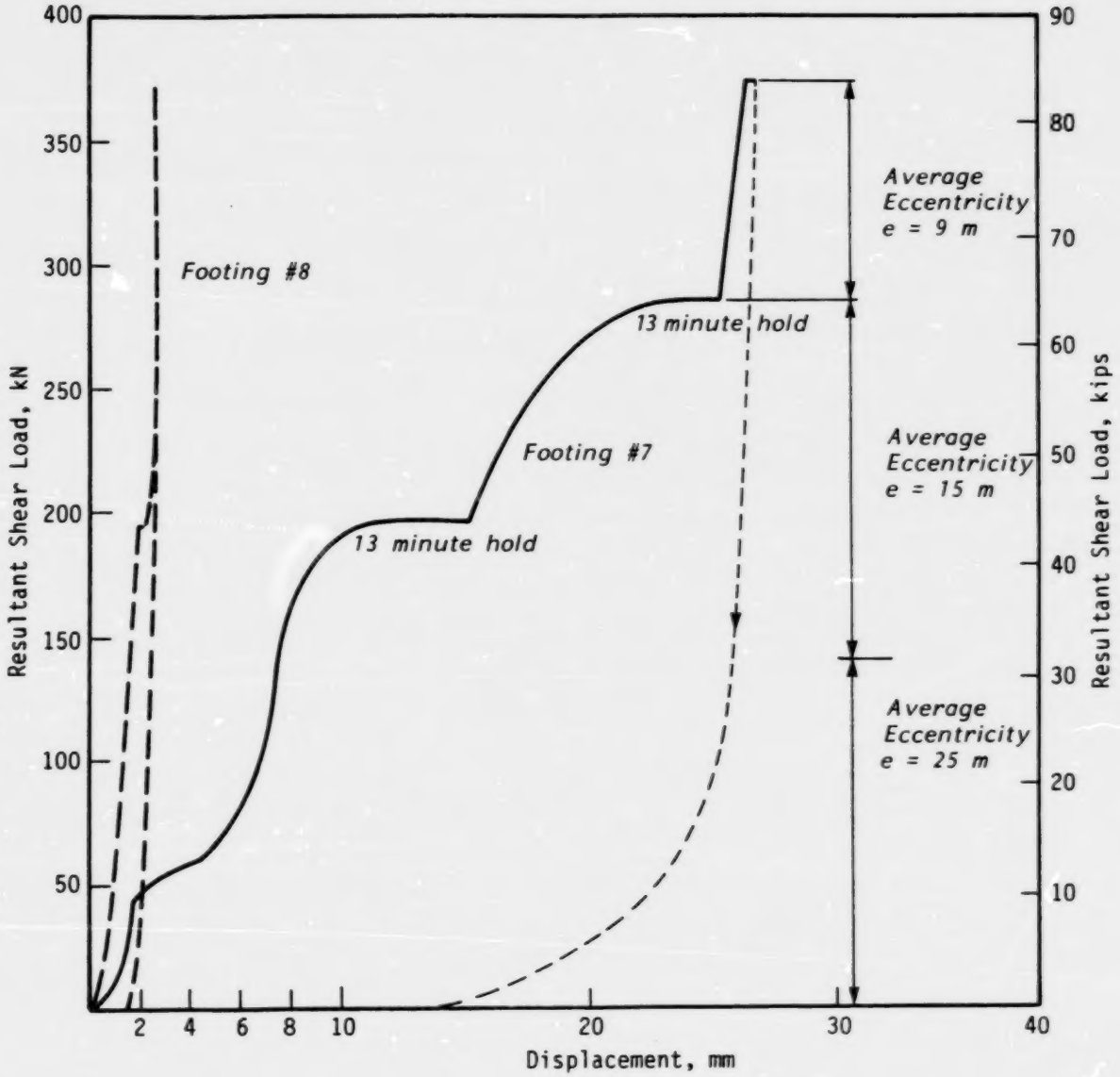

FIGURE 18

OVERTURNING MOMENT TEST BETWEEN FOOTING #7 AND #8
(WITH TOP & BOTTOM JACKS)

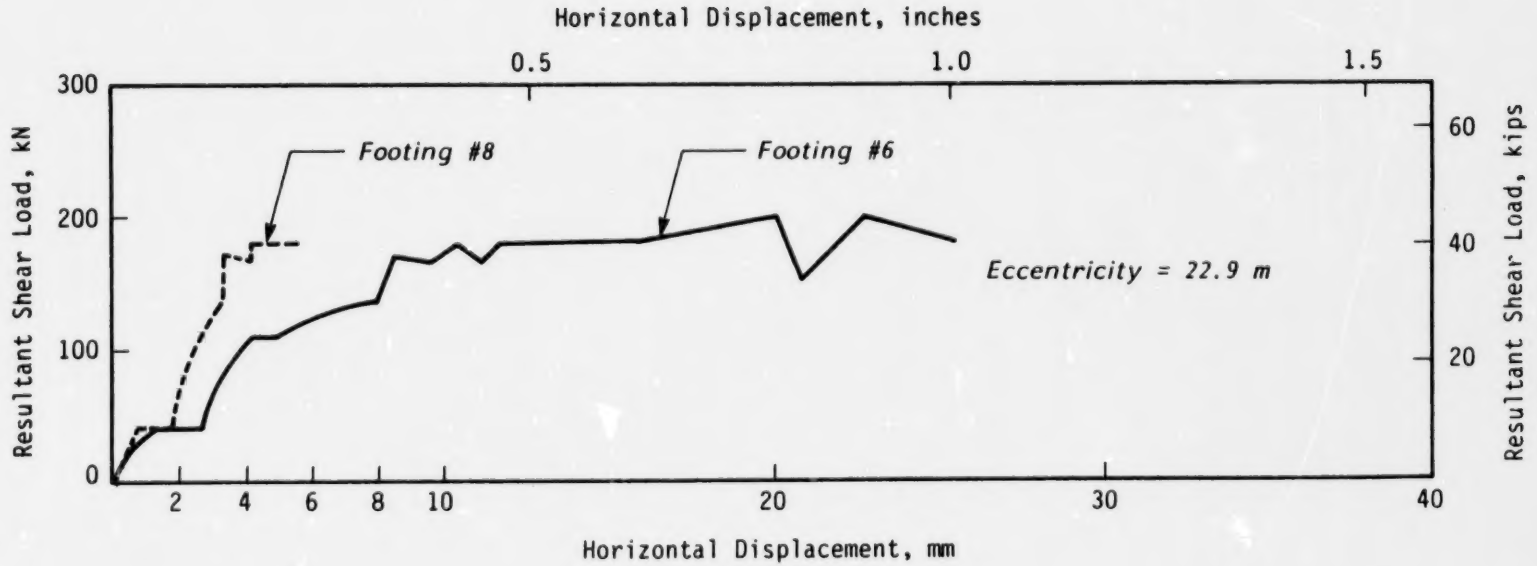

FIGURE 19

OVERTURNING MOMENT TEST BETWEEN FOOTINGS #6 AND #8
(WITH TOP AND BOTTOM JACKS)

87-19

170546 RD

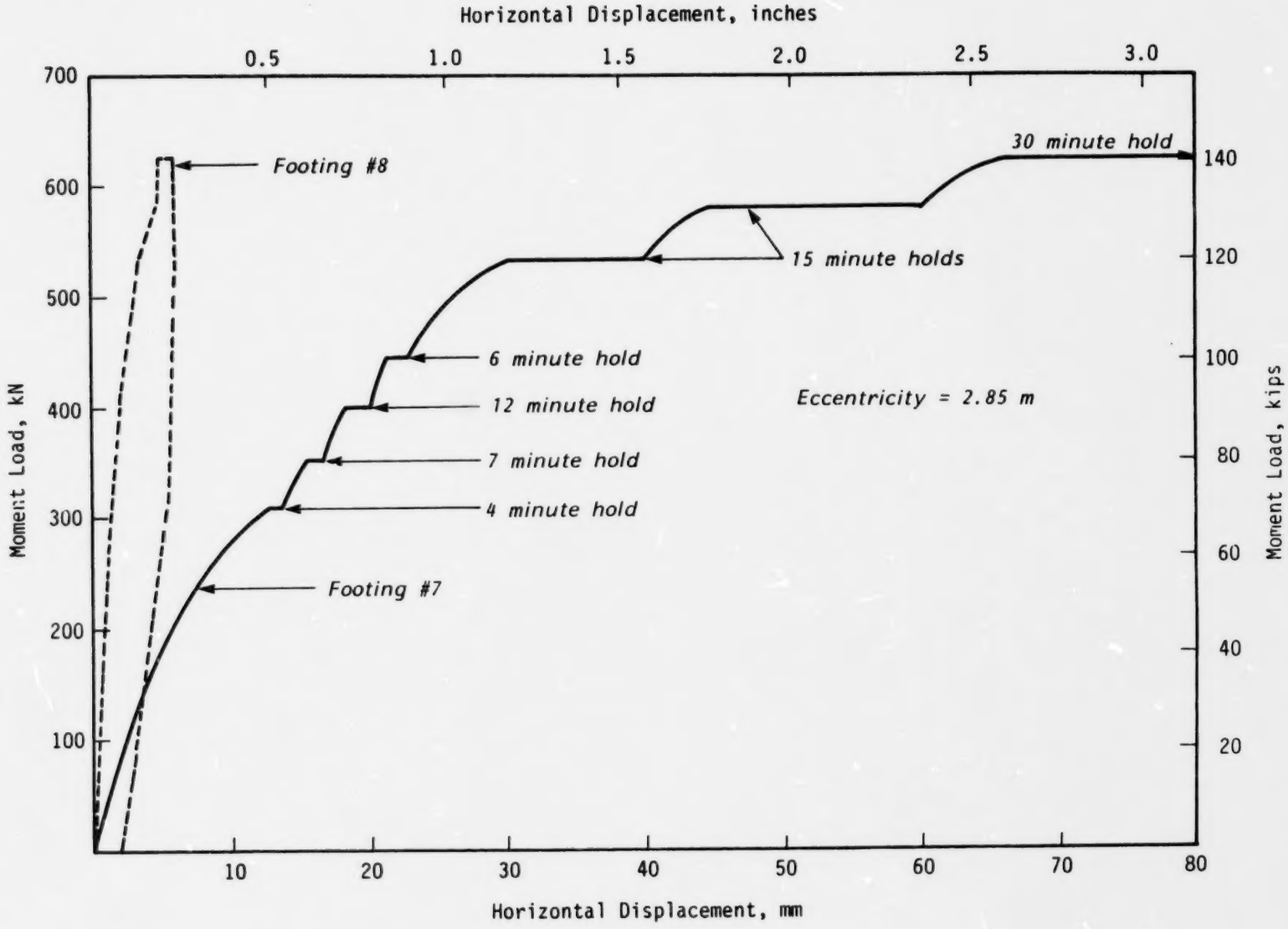

FIGURE 20

OVERTURNING MOMENT TEST BETWEEN FOOTING #7 AND #8 (WITHOUT BOTTOM JACK)

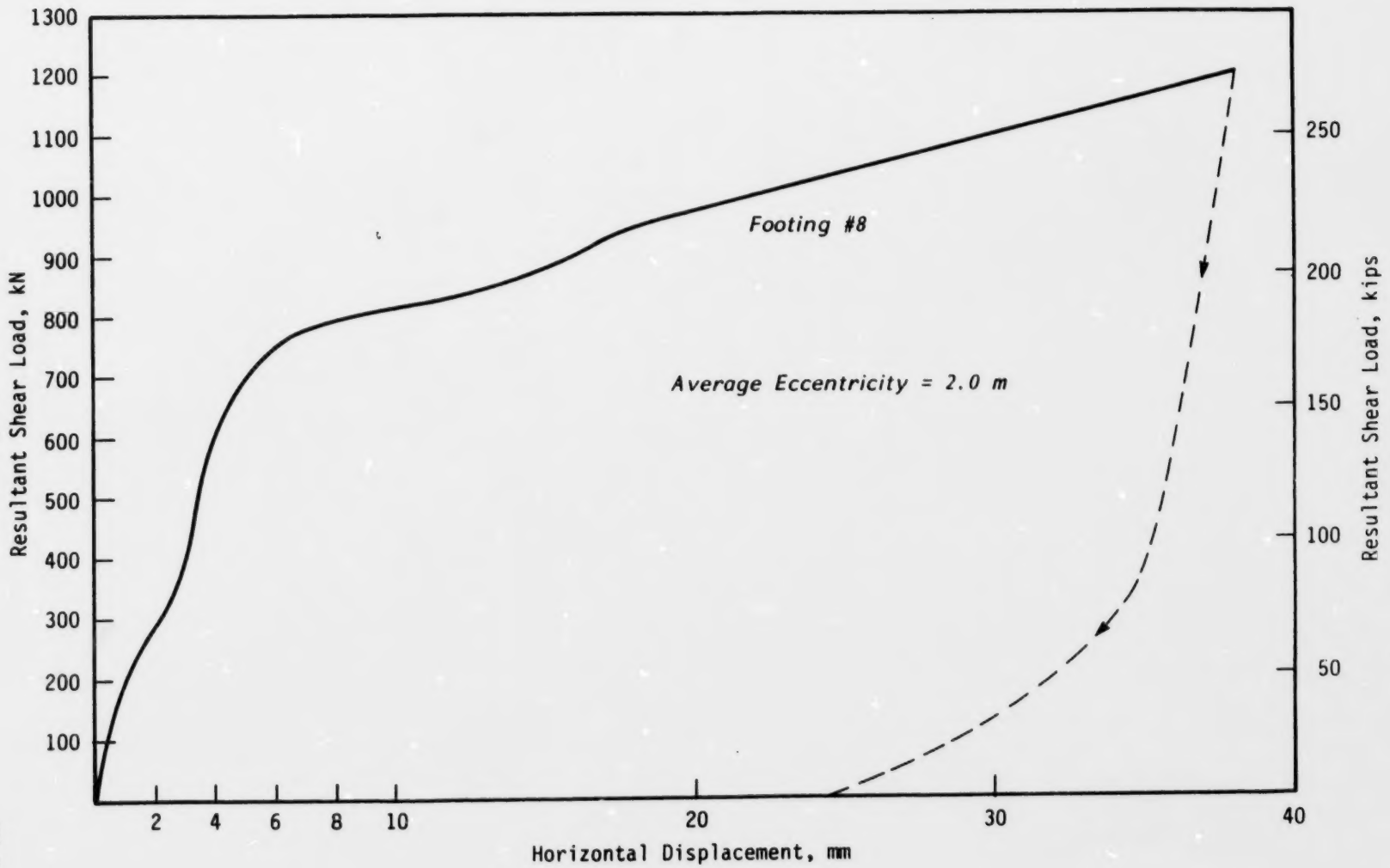

FIGURE 21

OVERTURNING MOMENT TEST BETWEEN FOOTINGS #6 AND #8
(WITH NO BOTTOM JACK)

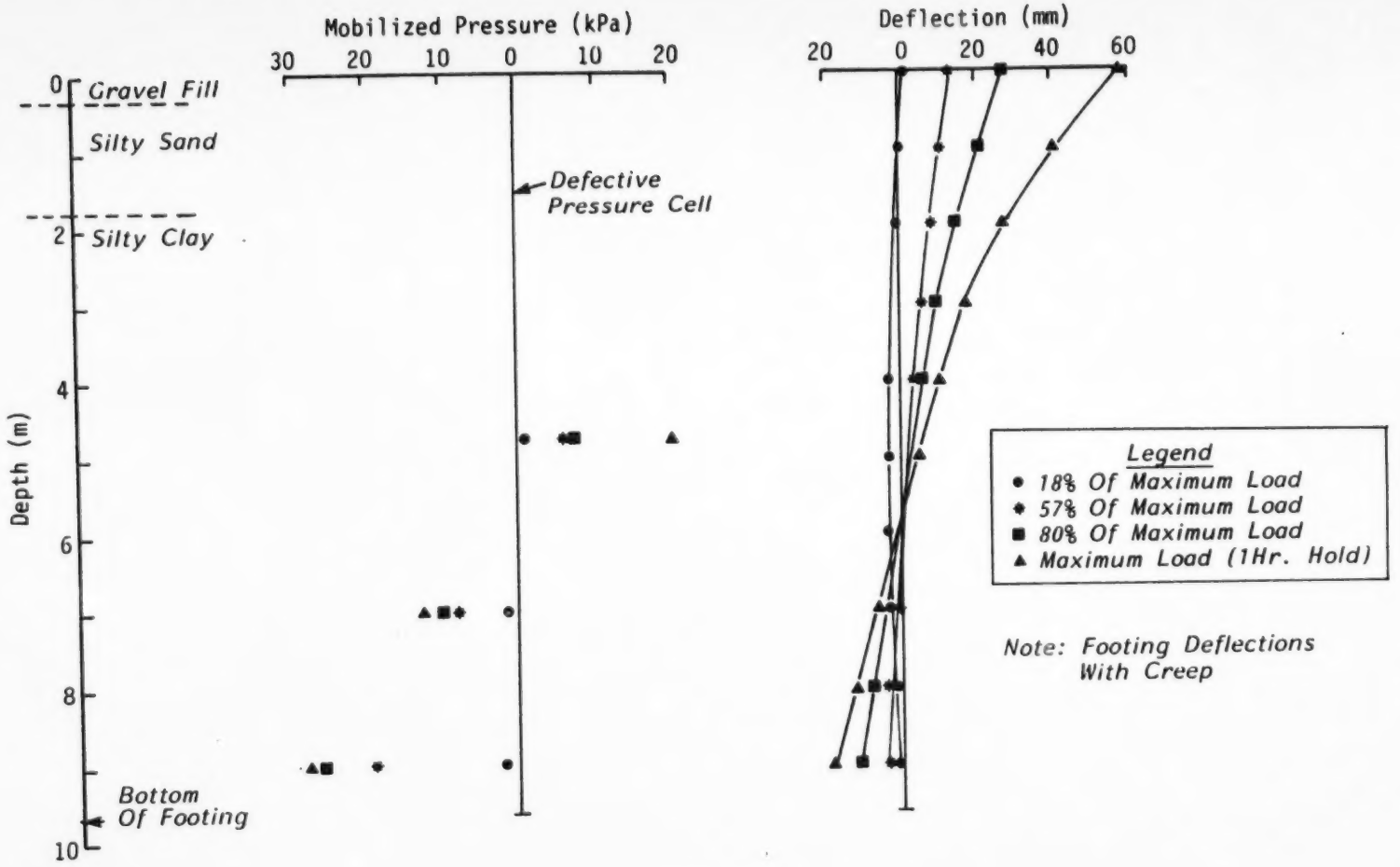

FIGURE 22

LATERAL LOAD TEST ON FOOTING 1
(0.93m DIA x 9.65m)

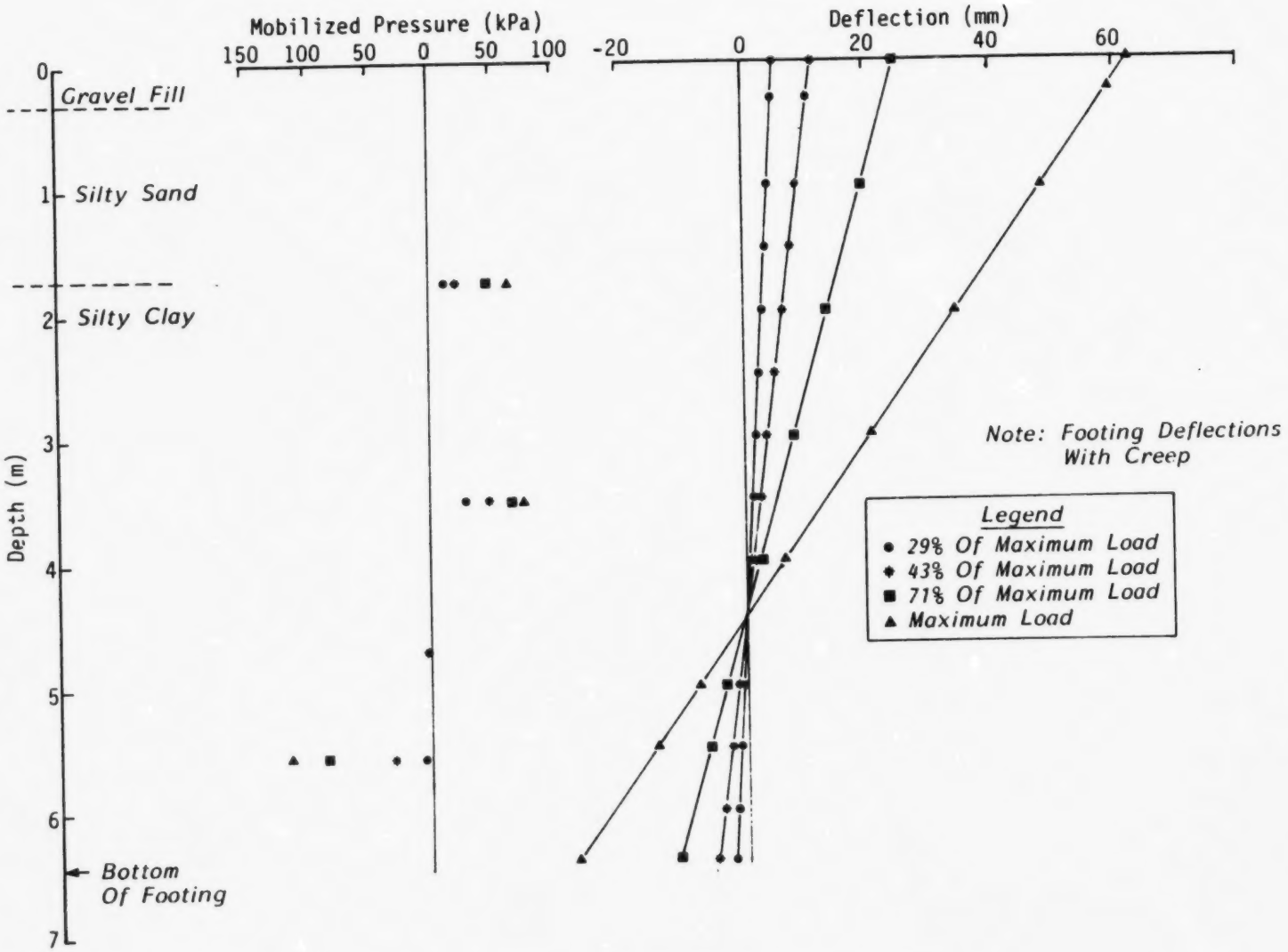

FIGURE 23

LATERAL LOAD TEST ON FOOTING #3
(1.50m DIA x 6.40m) TEST #6

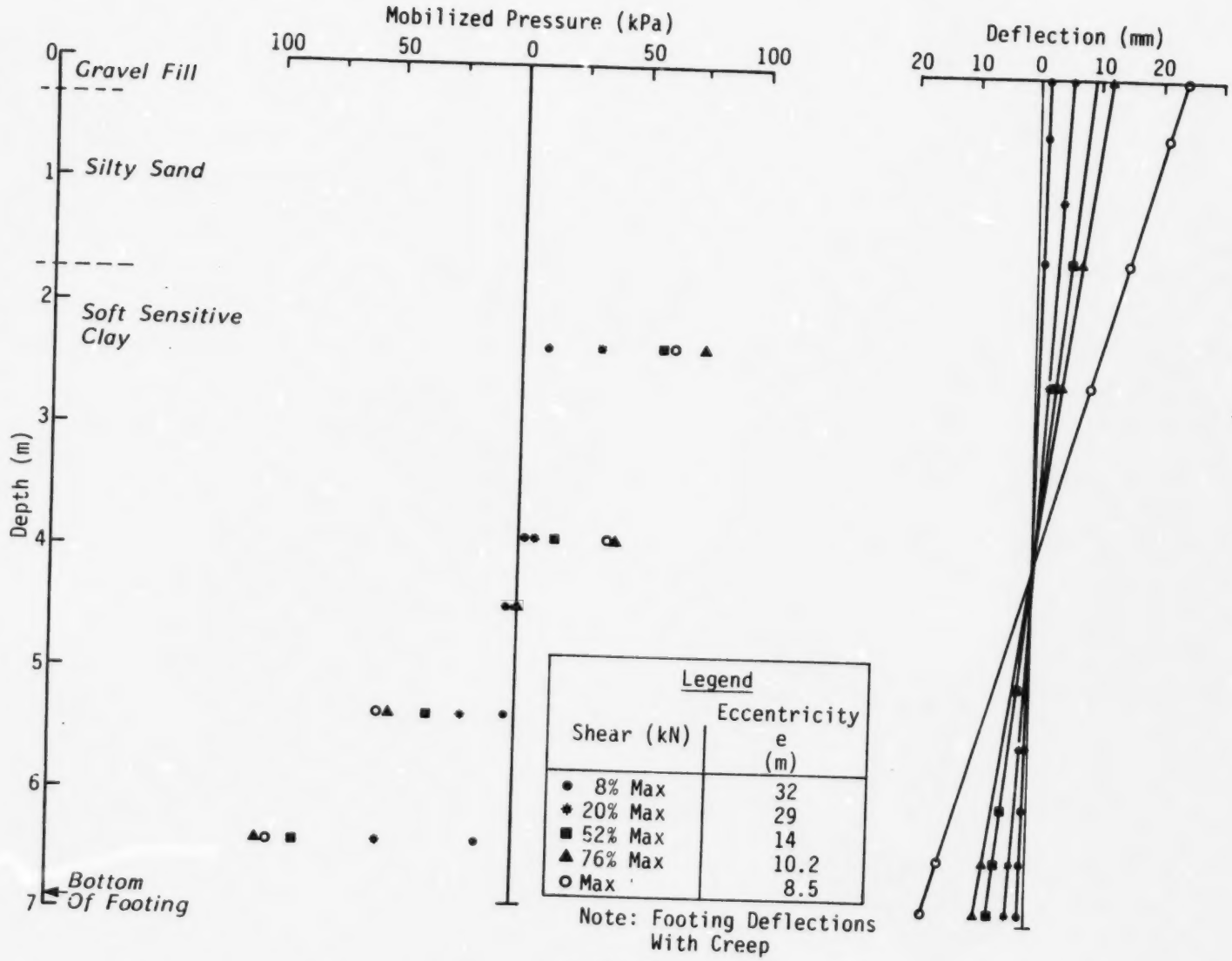

FIGURE 24
OVERTURNING MOMENT TEST ON FOOTING 7; DIA = 1.6m DEPTH = 6.9 WITH TOP AND BOTTOM JACKS (TEST 10a)

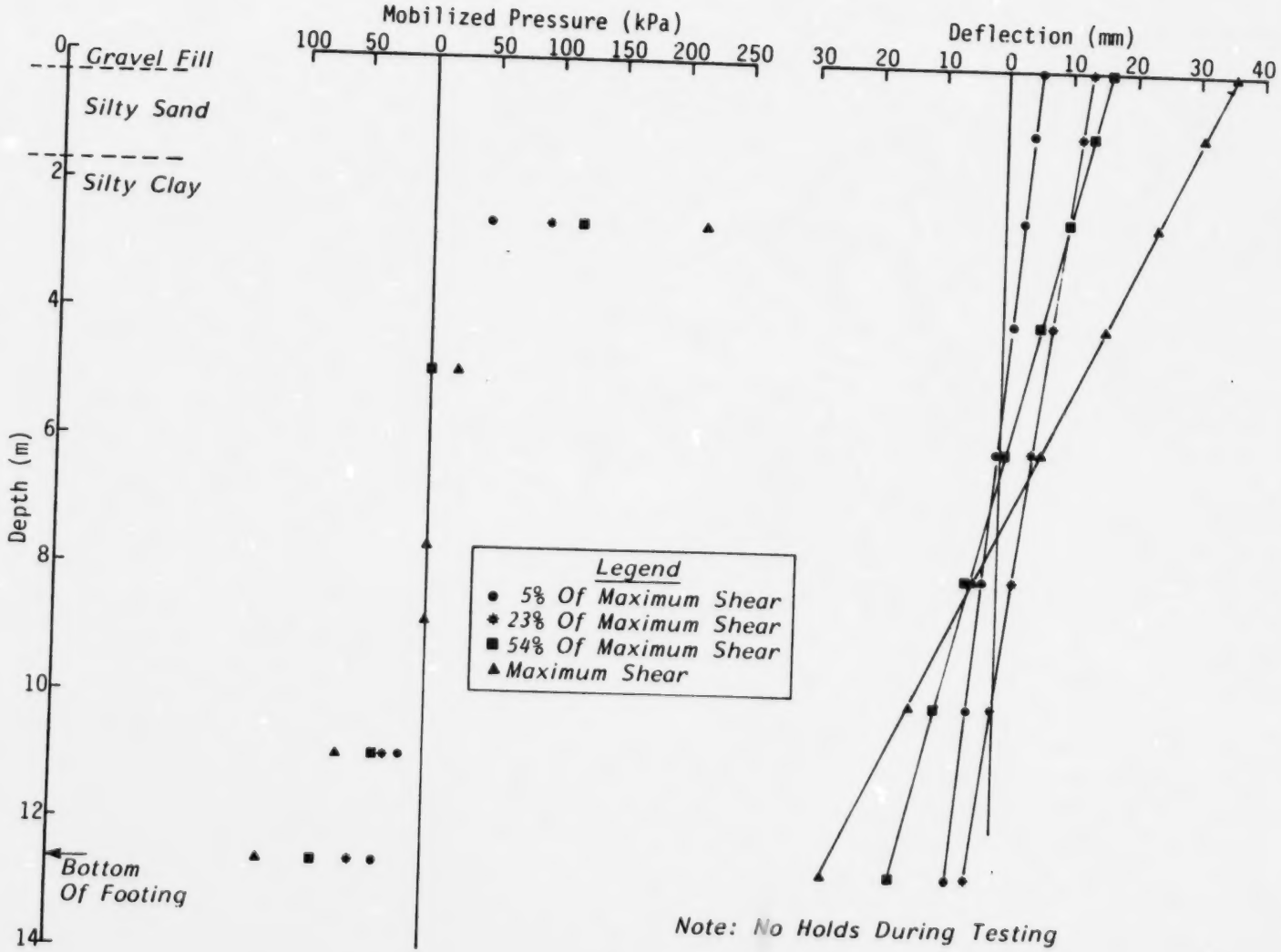

FIGURE 25
OVERTURNING MOMENT TEST ON FOOTING
#8 (2.76m DIA x 12.73m) WITH TOP
JACKS ONLY (TEST #12)

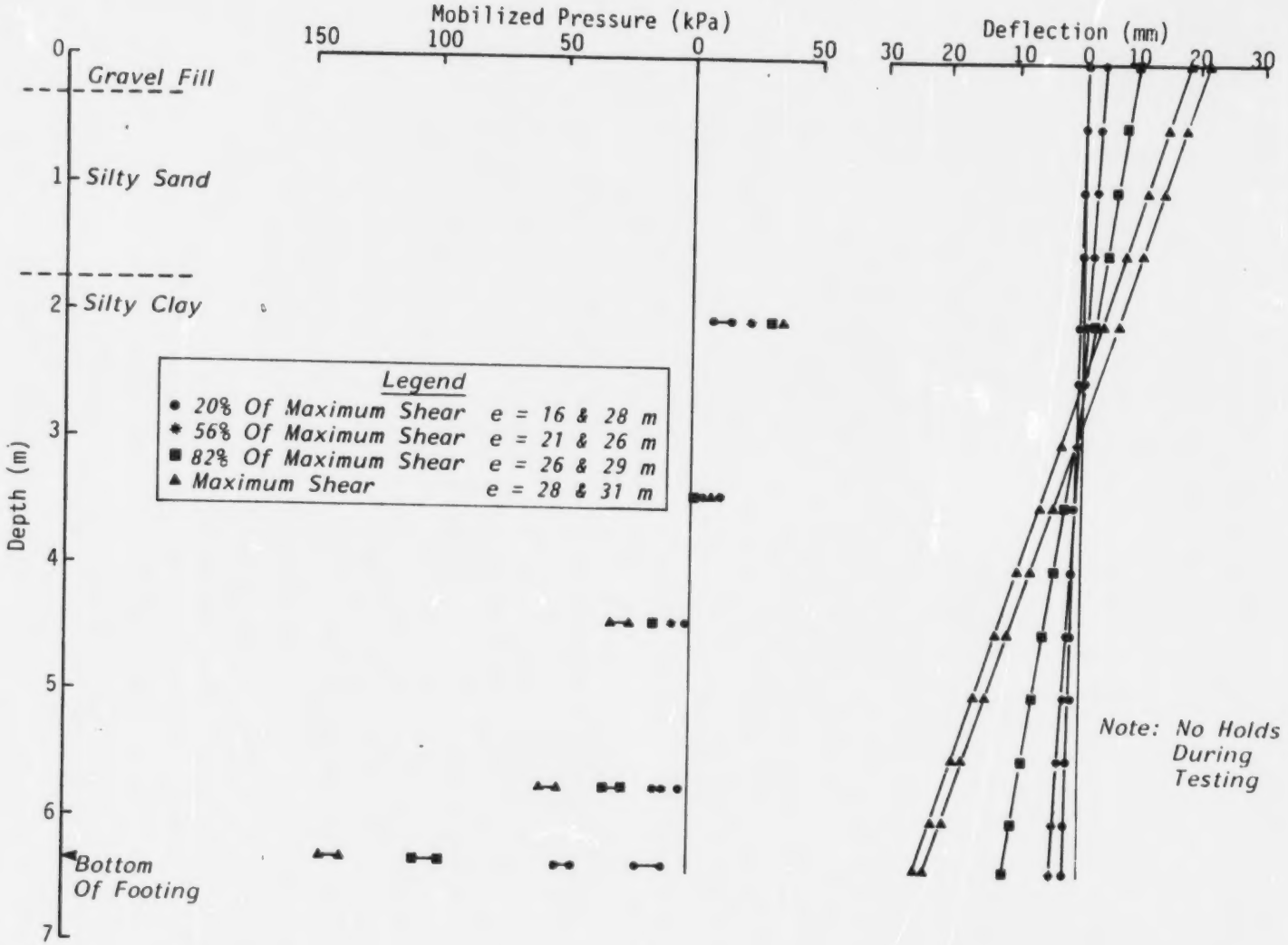

FIGURE 26
OVERTURNING MOMENT TEST ON FOOTING
#6 (2.49m DIA x 6.63m)
WITH TOP AND BOTTOM JACKS (TEST #11)

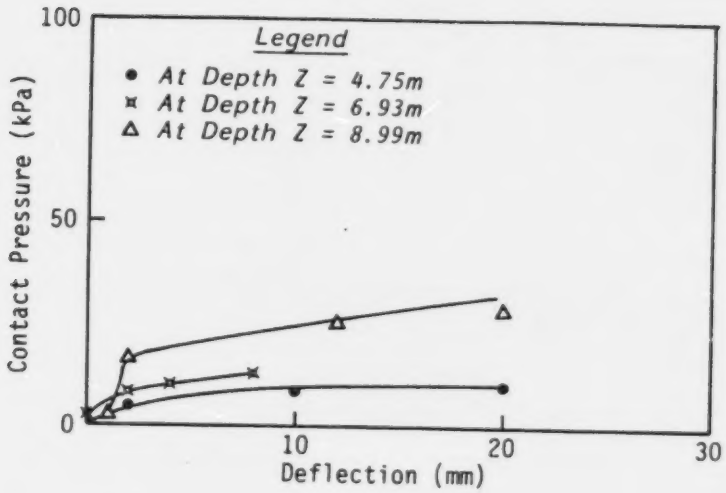

Note *Pressure Cell At Z = 1.70m Defective*

FIGURE 27

(p-y) CURVES FROM LATERAL LOAD TEST ON FOOTING #1 (0.93m $\overline{\text{DIA}}$ x 9.65m)

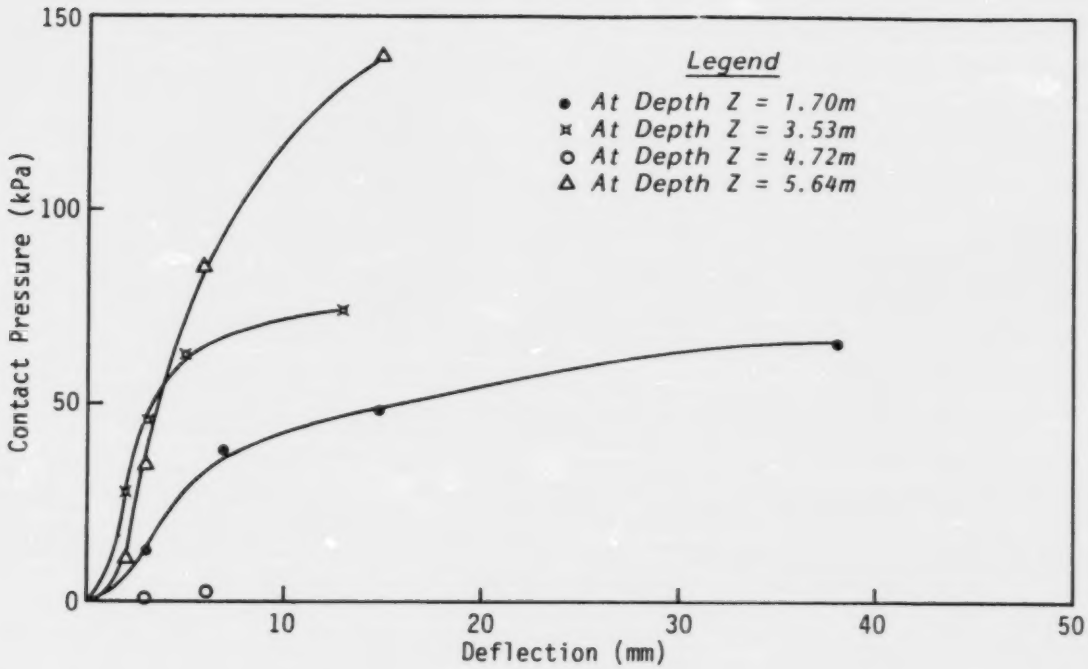

FIGURE 28

(p-y) CURVES FROM LATERAL LOAD TEST ON FOOTING 3 (1.50m $\overline{\text{DIA}}$ x 6.40m)

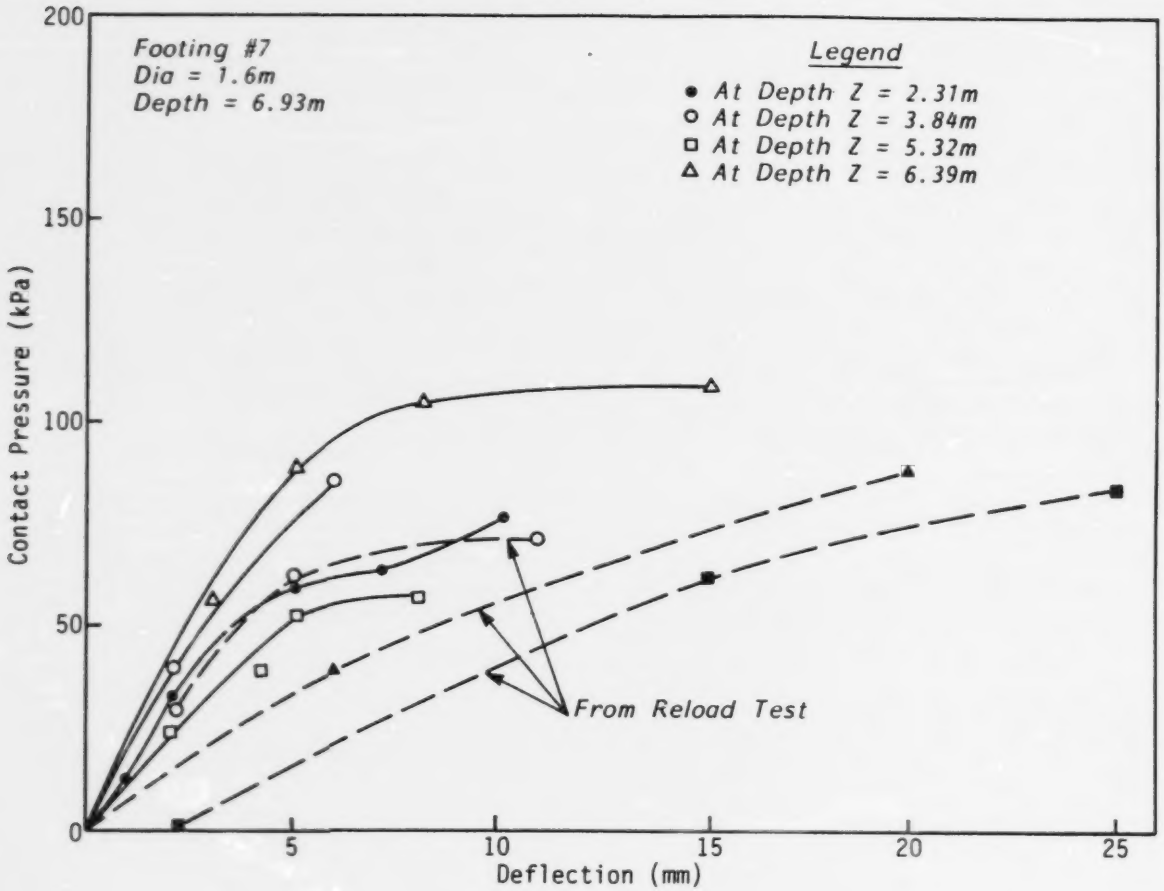

FIGURE 29

(p-y) CURVES FROM OVERTURNING MOMENT TEST ON FOOTING #7

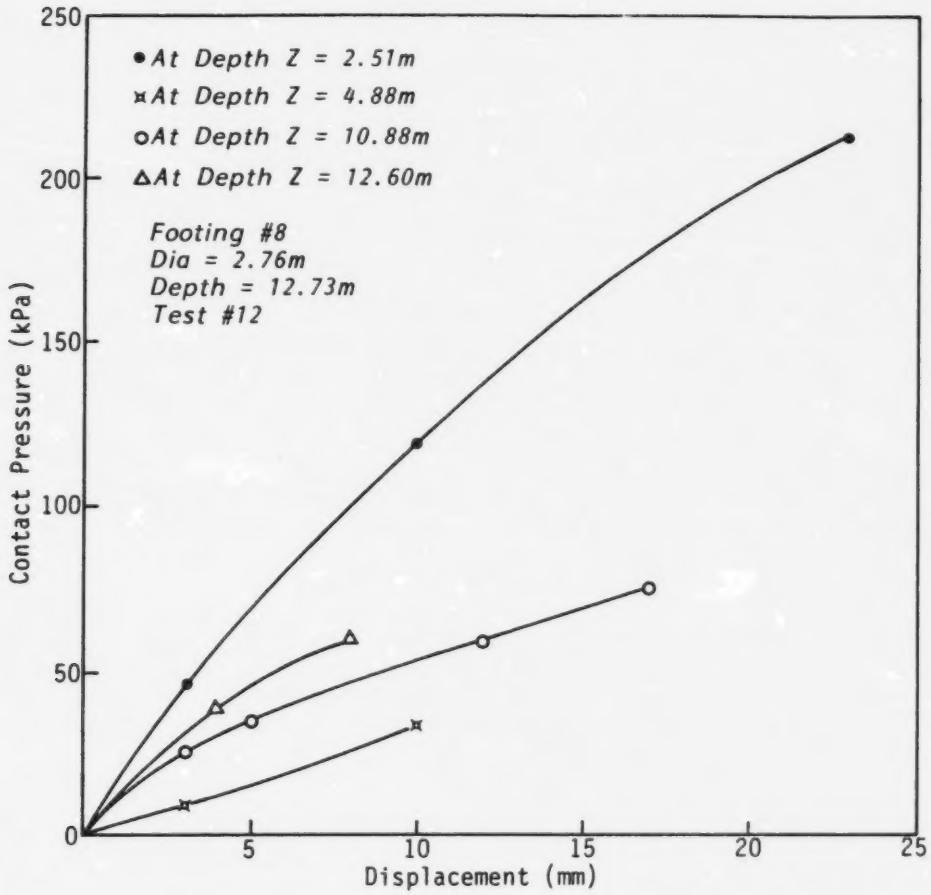

FIGURE 30

(p-y) CURVES FROM OVERTURNING MOMENT TEST ON FOOTING #8

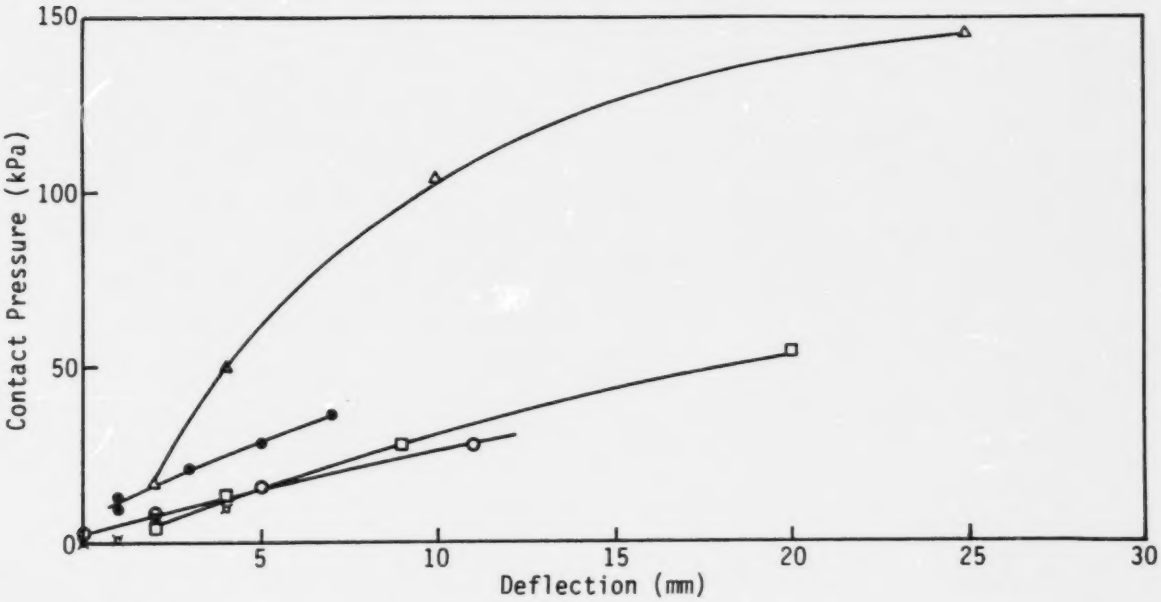

Legend

- ● *At Depth Z = 2.13m*
- ✕ *At Depth Z = 3.44m*
- ○ *At Depth Z = 4.42m*
- □ *At Depth Z = 5.75m*
- △ *At Depth Z = 6.39m*

FIGURE 31

(p-y) CURVES FROM OVERTURNING MOMENT TEST ON FOOTING #6
(2.49m $\overline{\text{DIA}}$ x 6.63m) WITH TOP AND BOTTOM JACKS

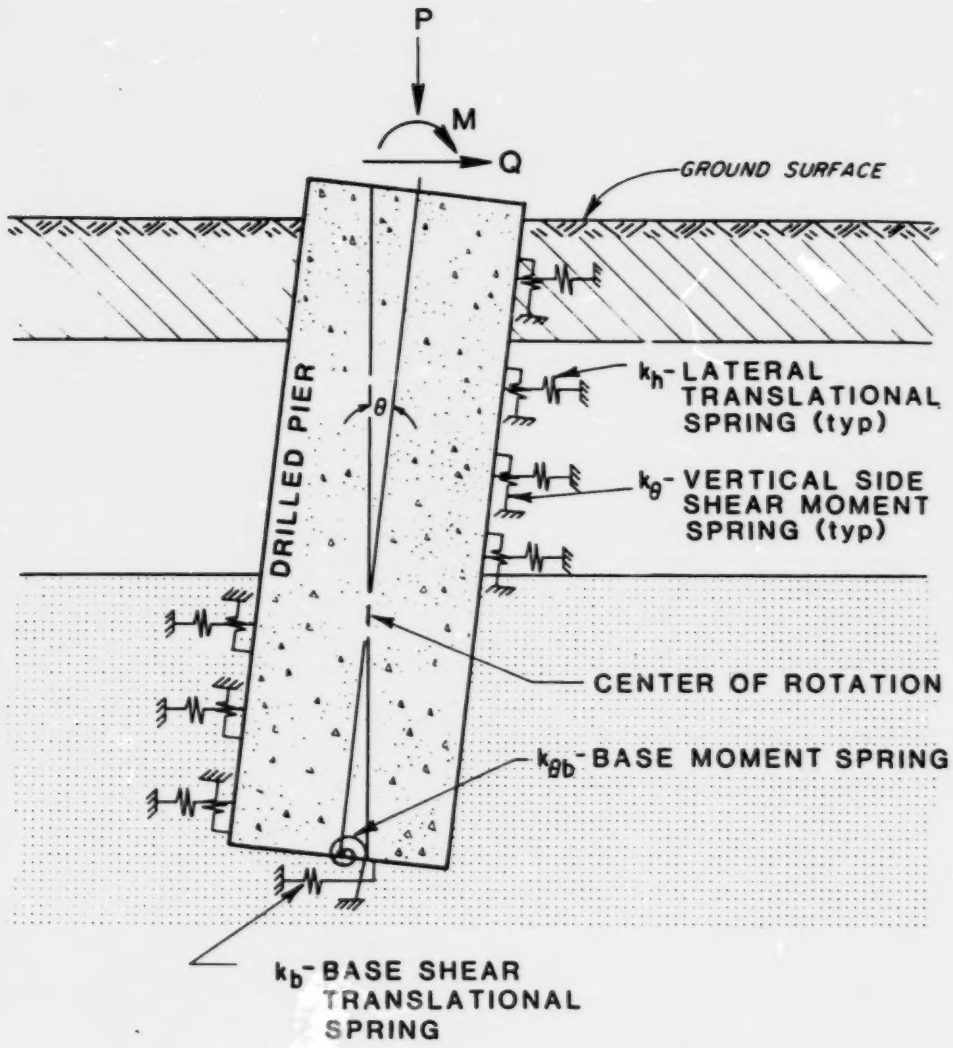

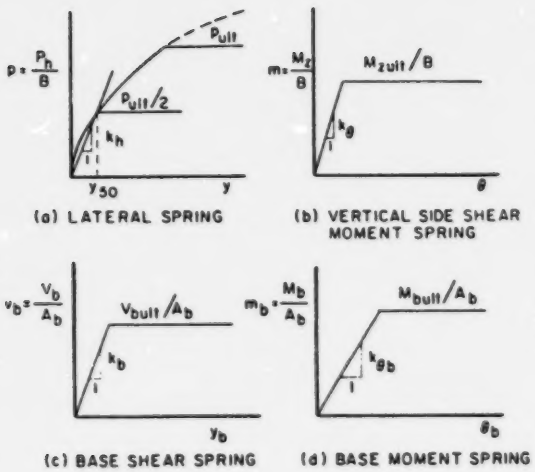

(a) LATERAL SPRING

(b) VERTICAL SIDE SHEAR MOMENT SPRING

(c) BASE SHEAR SPRING

(d) BASE MOMENT SPRING

FIGURE 32
FOUR SPRING MODEL FOR LATERALLY LOADED PIER FOUNDATION USED IN PADLL PROGRAM (DAVIDSON 1982)

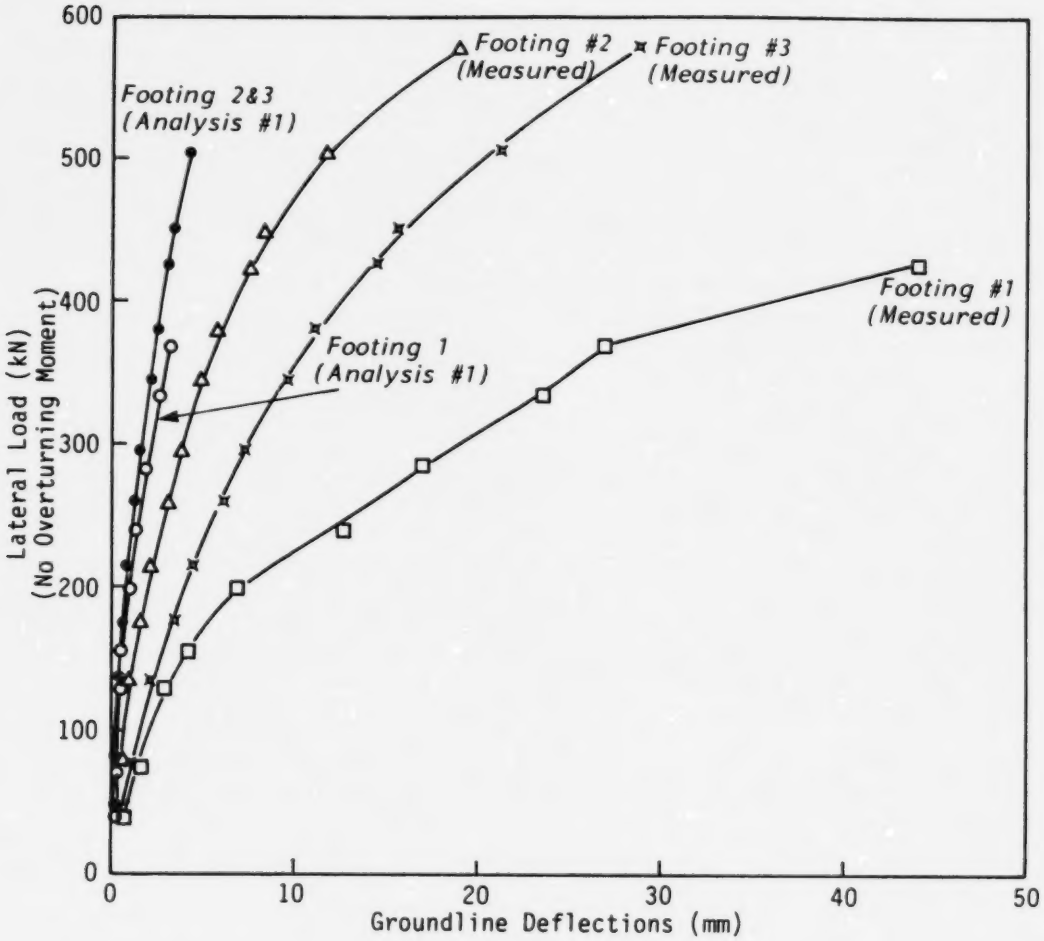

FIGURE 33

COMPARISON BETWEEN MEASURED AND PREDICTED DEFLECTIONS
FOOTINGS 1, 2 AND 3 (ANALYSIS #1)

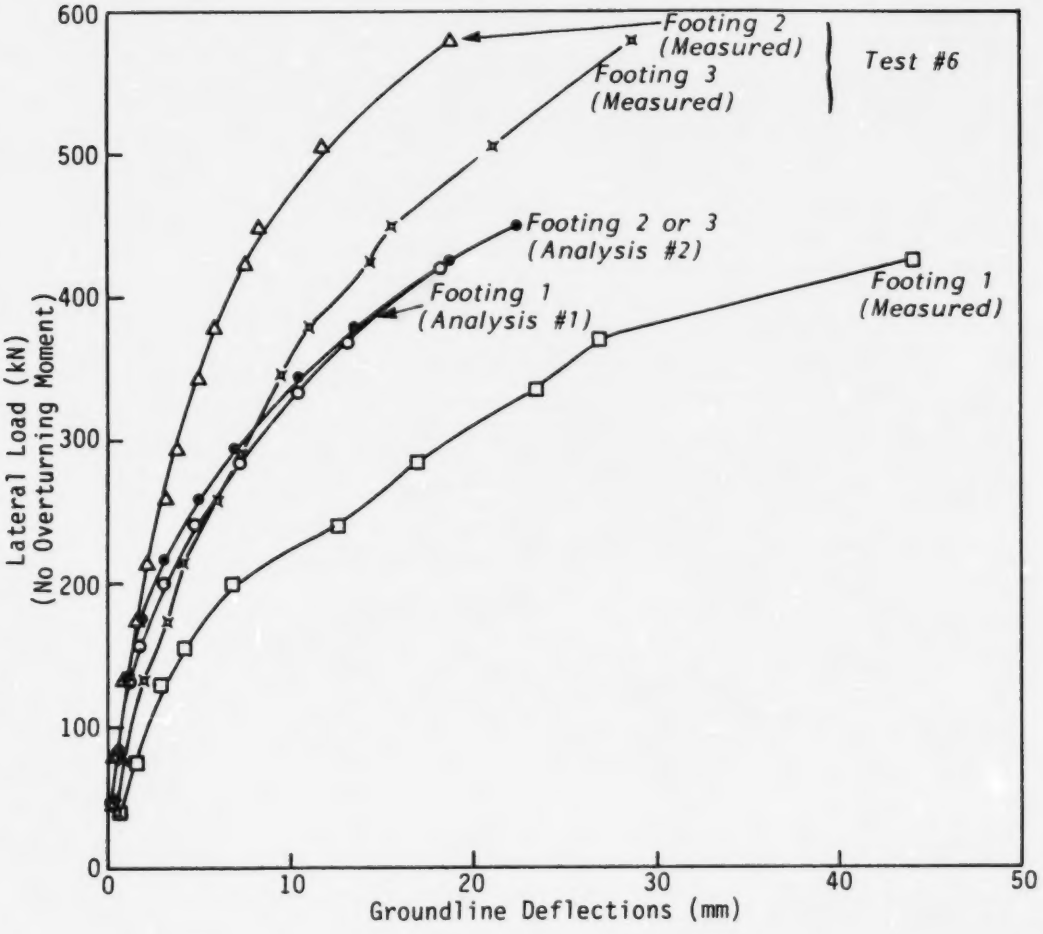

FIGURE 34

COMPARISON BETWEEN MEASURED AND PREDICTED
DEFLECTIONS FOR FOOTINGS 1, 2 AND 3 (ANALYSIS #2)

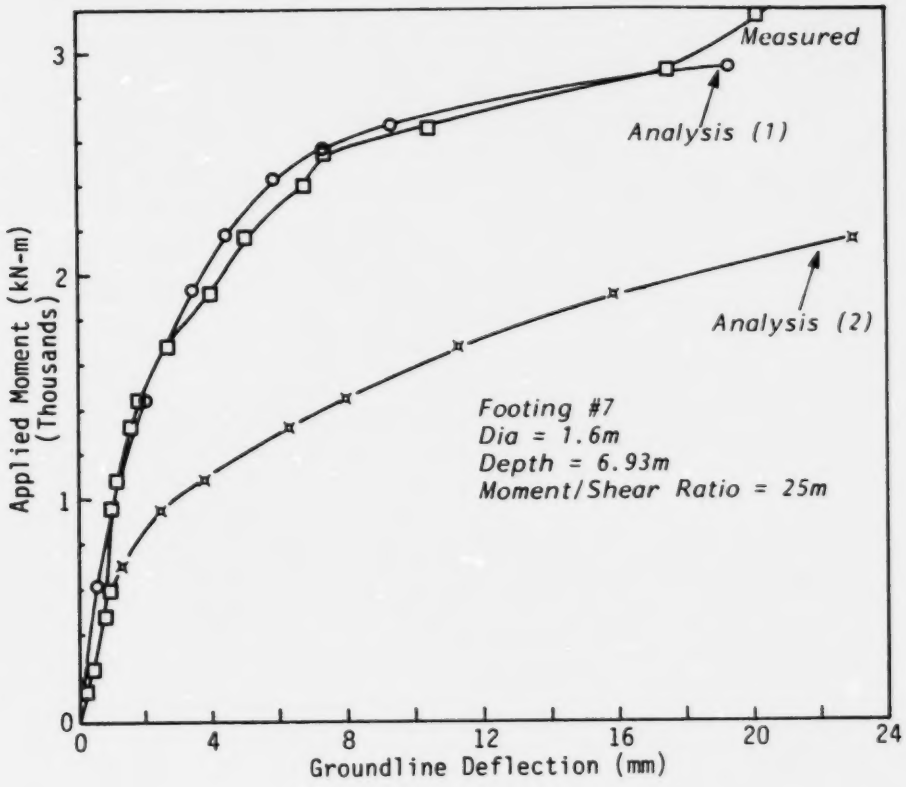

FIGURE 35

COMPARISON BETWEEN MEASURED AND PREDICTED
LOAD-DEFLECTION RESPONSE OF FOOTING 7 (TEST#9)

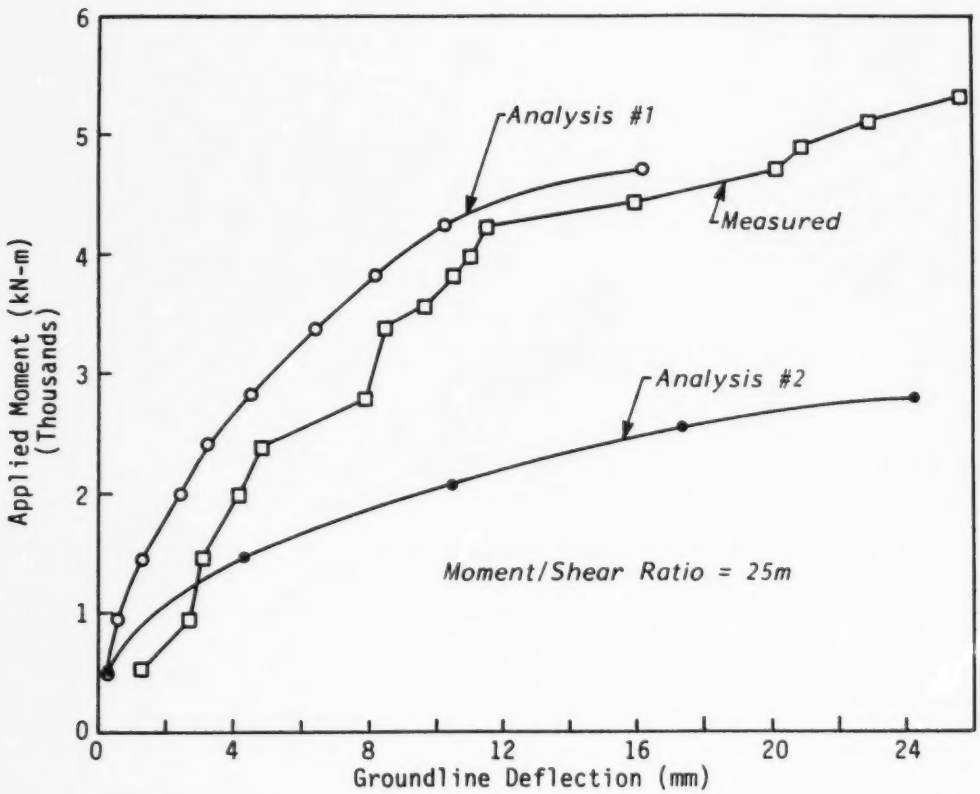

FIGURE 36

COMPARISON BETWEEN MEASURED AND PREDICTED
LOAD-DEFLECTION RESPONSE OF FOOTING 6 (TEST#11)

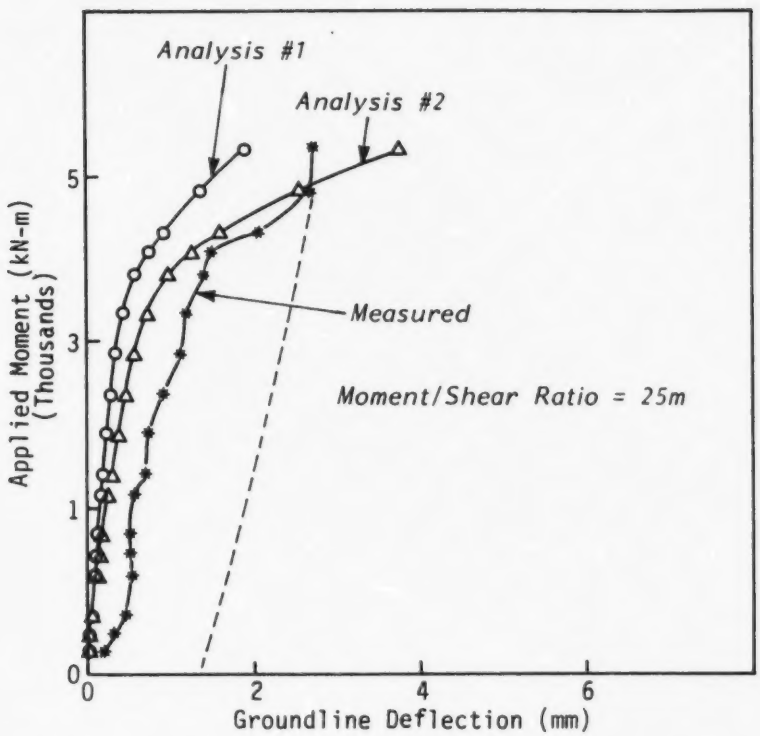

FIGURE 37

COMPARISON BETWEEN MEASURED AND PREDICTED
LOAD-DEFLECTION RESPONSE OF FOOTING 8 (TEST#9)

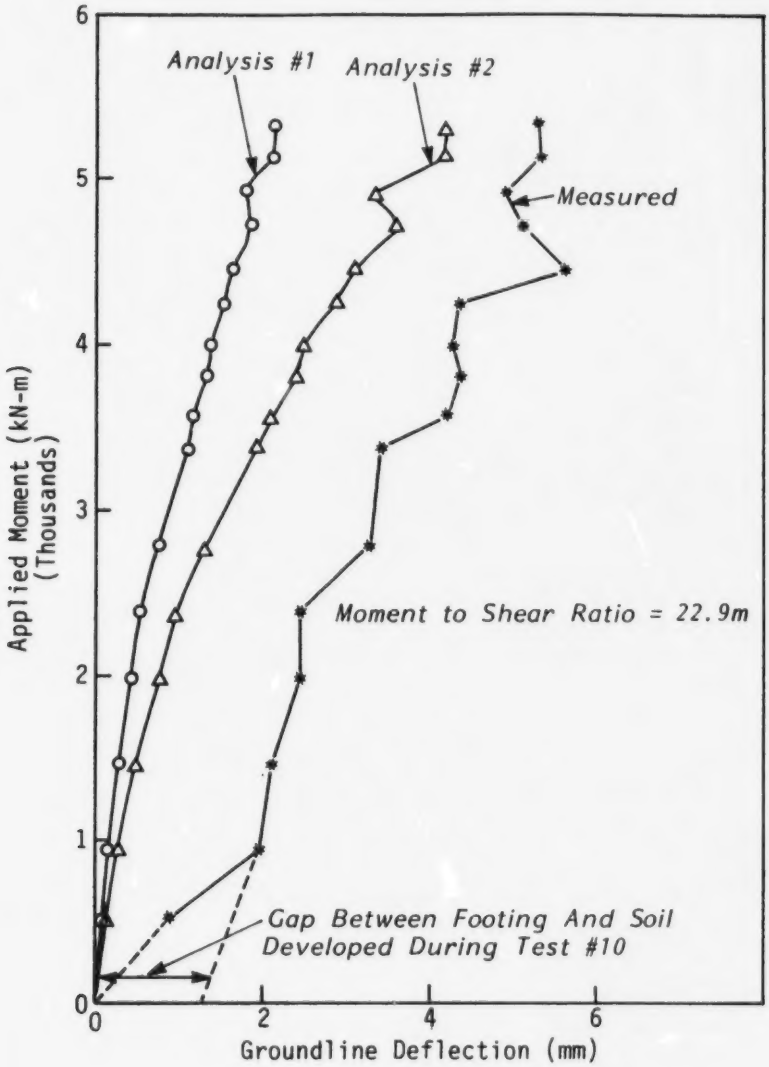

FIGURE 38

COMPARISON BETWEEN MEASURED AND PREDICTED
LOAD-DEFLECTION RESPONSE FOR FOOTING 8 (TEST 11)

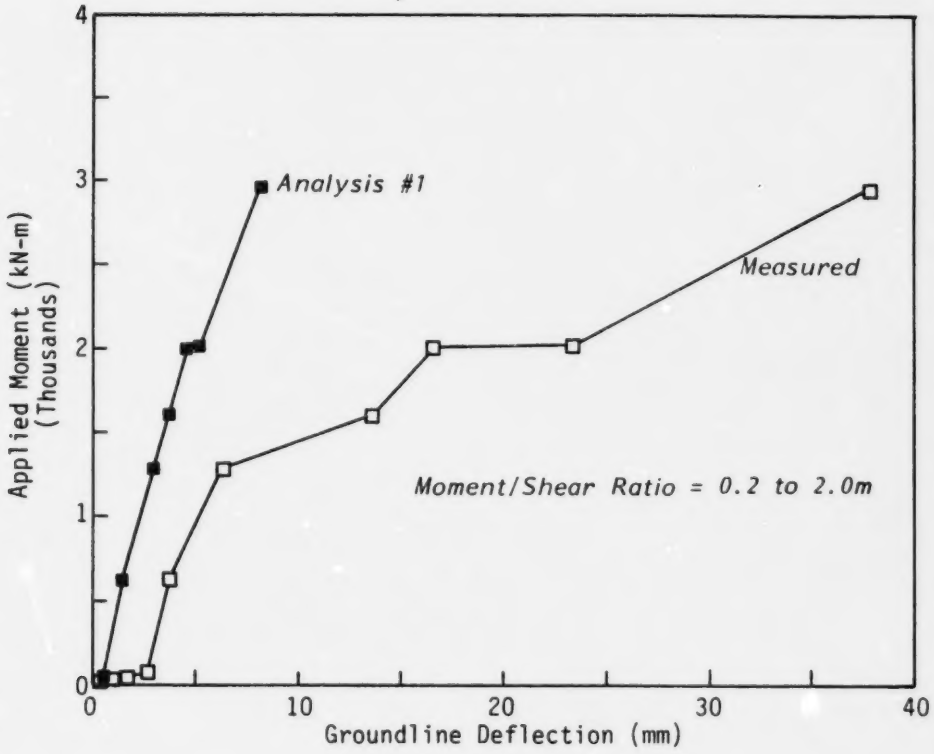

FIGURE 39

COMPARISON BETWEEN MEASURED AND PREDICTED
LOAD-DEFLECTION RESPONSE OF FOOTING #8 (TEST#12)

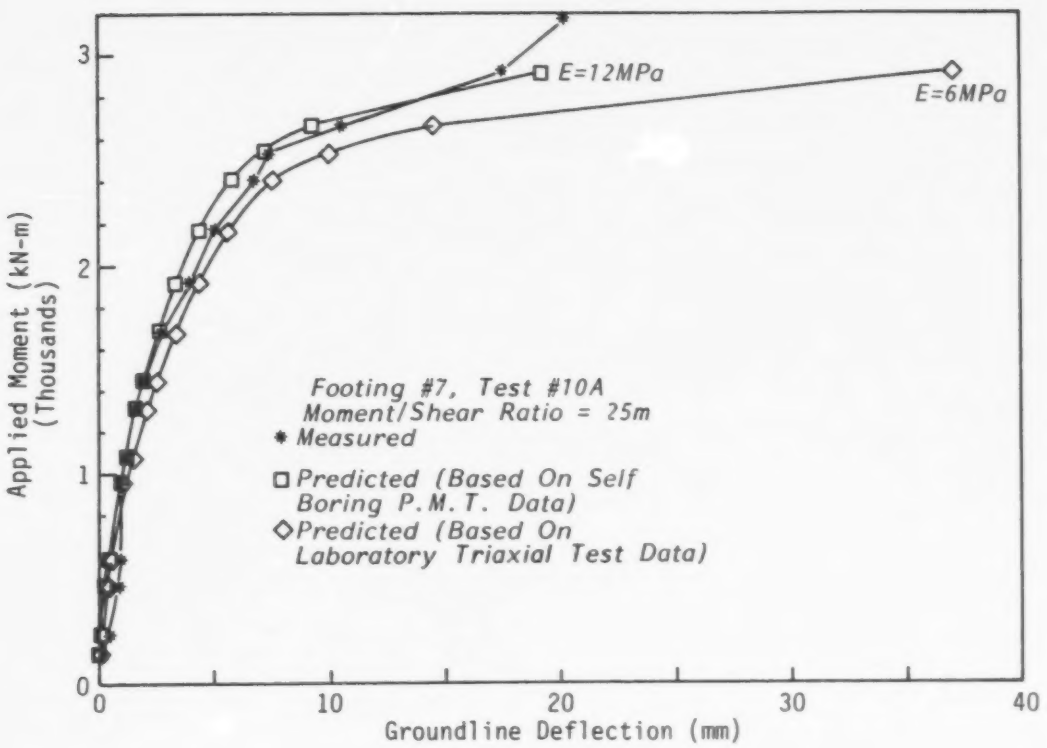

FIGURE 40

SENSITIVITY OF PREDICTED LOAD-DEFLECTION RESPONSE BY PADLL PROGRAM TO INPUT MODULUS VALUES FOR LEDA CLAY IN ANALYSIS #1

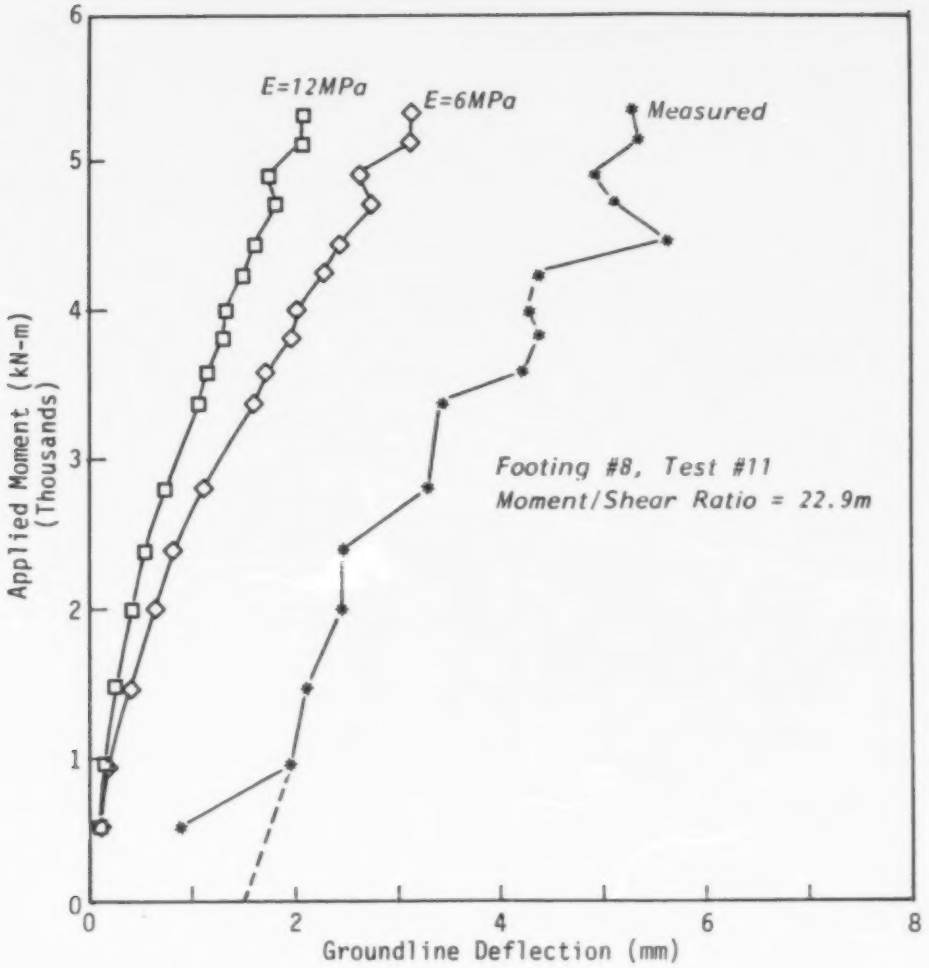

FIGURE 41

SENSITIVITY OF PREDICTED LOAD-DEFLECTION RESPONSE BY PADLL PROGRAM TO INPUT MODULUS VALUES FOR LEDA CLAY IN ANALYSIS #1

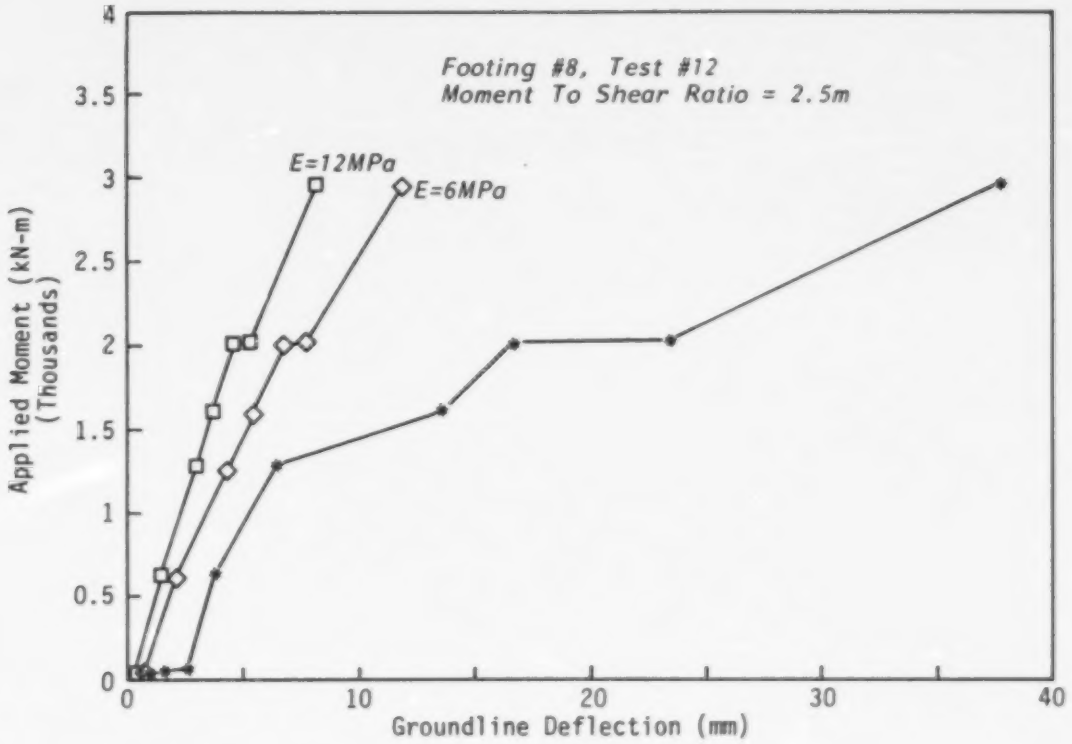

FIGURE 42

SENSITIVITY OF PREDICTED LOAD-DEFLECTION RESPONSE BY PADLL PROGRAM TO INPUT MODULUS VALUES FOR LEDA CLAY IN ANALYSIS #1

APPENDIX A

Instrumentation of Test Footings

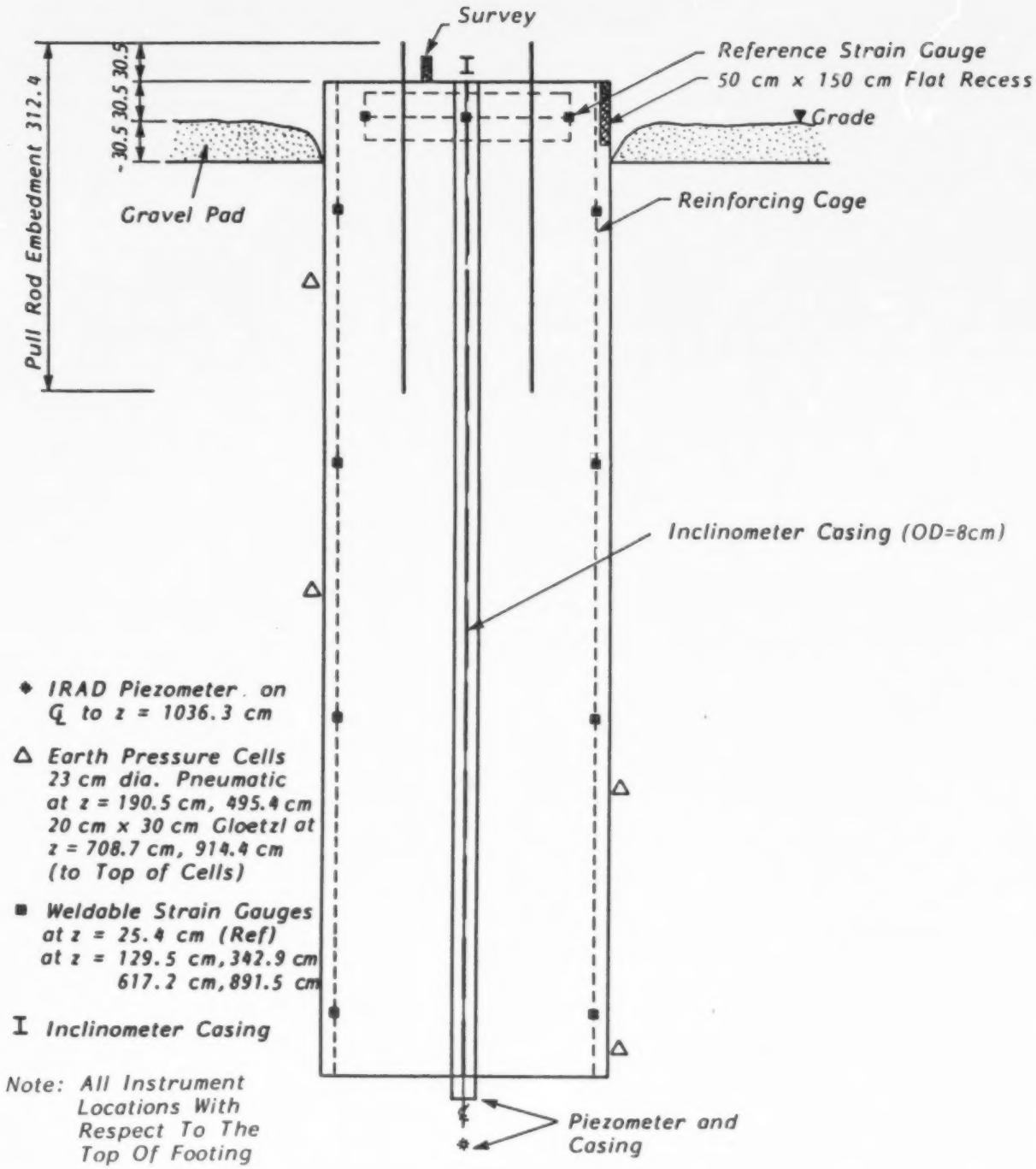
Survey
Reference Strain Gauge
50 cm x 150 cm Flat Recess
Grade
Reinforcing Cage
Gravel Pad
-30.5 30.5 30.5
Pull Rod Embedment 312.4
Inclinometer Casing (OD=8cm)
IRAD Piezometer on ℄ to z = 1036.3 cm
Earth Pressure Cells 23 cm dia. Pneumatic at z = 190.5 cm, 495.4 cm 20 cm x 30 cm Gloetzl at z = 708.7 cm, 914.4 cm (to Top of Cells)
Weldable Strain Gauges at z = 25.4 cm (Ref) at z = 129.5 cm, 342.9 cm 617.2 cm, 891.5 cm
Inclinometer Casing
Note: All Instrument Locations With Respect To The Top Of Footing
Piezometer and Casing

FIGURE A1

INSTRUMENTATION OF TEST FOOTING #1

0.92 m Average Diameter by 9.65 m Embedded Length

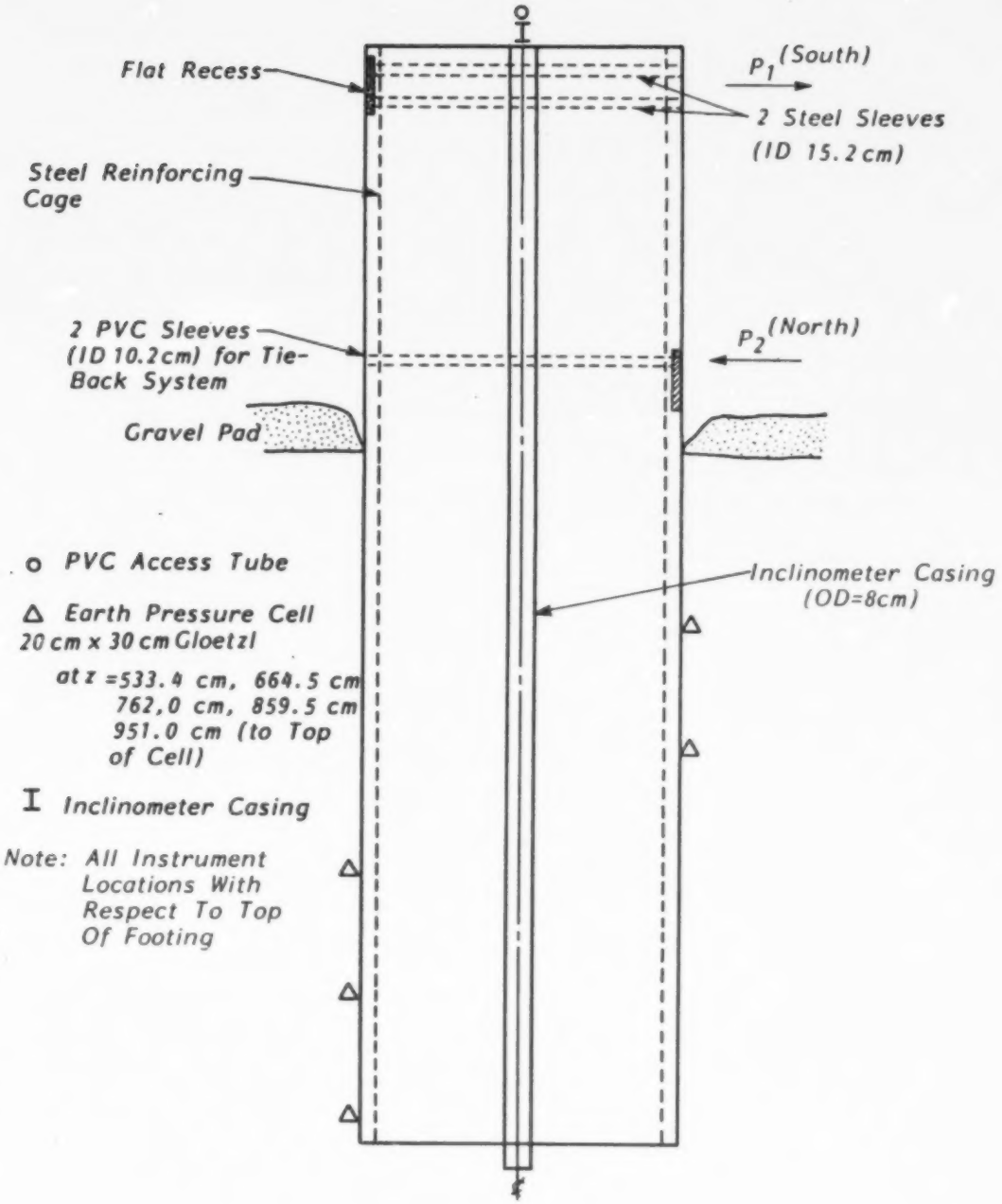

FIGURE A2

INSTRUMENTATION OF TEST FOOTING #6

2.49 m Average Diameter x 6.63 m Embedded Length

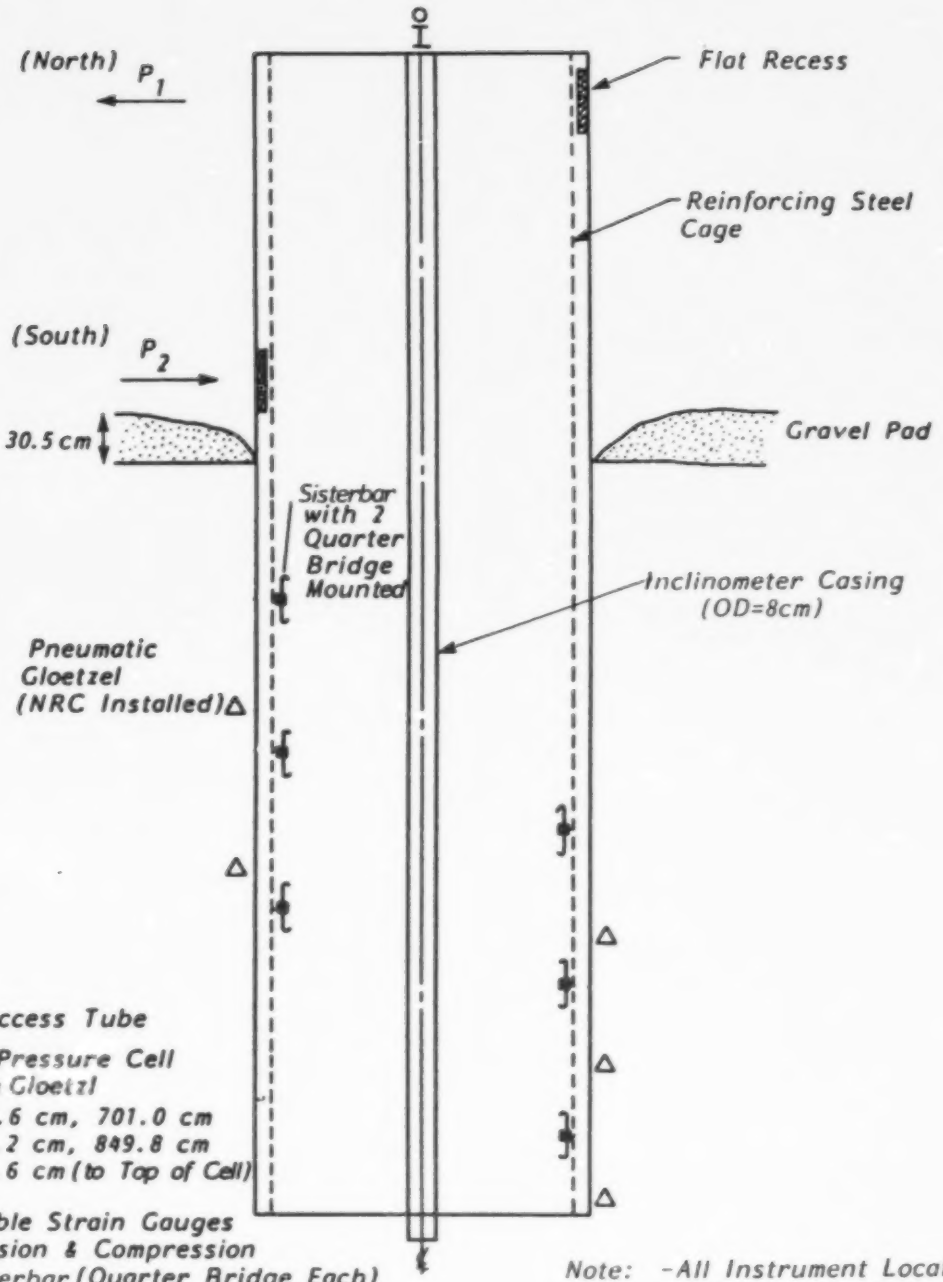
(North) P_1
Flat Recess
Reinforcing Steel Cage
(South) P_2
30.5 cm
Gravel Pad
Sisterbar with 2 Quarter Bridge Mounted
Inclinometer Casing (OD=8cm)
Pneumatic Gloetzel (NRC Installed)
o PVC Access Tube
Δ Earth Pressure Cell 20 cm x 30 cm Gloetzl at z=548.6 cm, 701.0 cm 753.2 cm, 849.8 cm 956.6 cm (to Top of Cell)
2 Weldable Strain Gauges for Tension & Compression per Sisterbar (Quarter Bridge Each)
at z=487.7 cm, 609.6 cm 670.6 cm, 730.5 cm 792.5 cm, 914.4 cm
I Inclinometer Casing
Note: -All Instrument Locations With Respect To Top Of Footing
-All Strain Gauges Offset 17 cm From ℄ Axis Of Footing

FIGURE A3

INSTRUMENTATION OF TEST FOOTING #7

1.60 m Average Diameter x 6.93 m Embedded Length

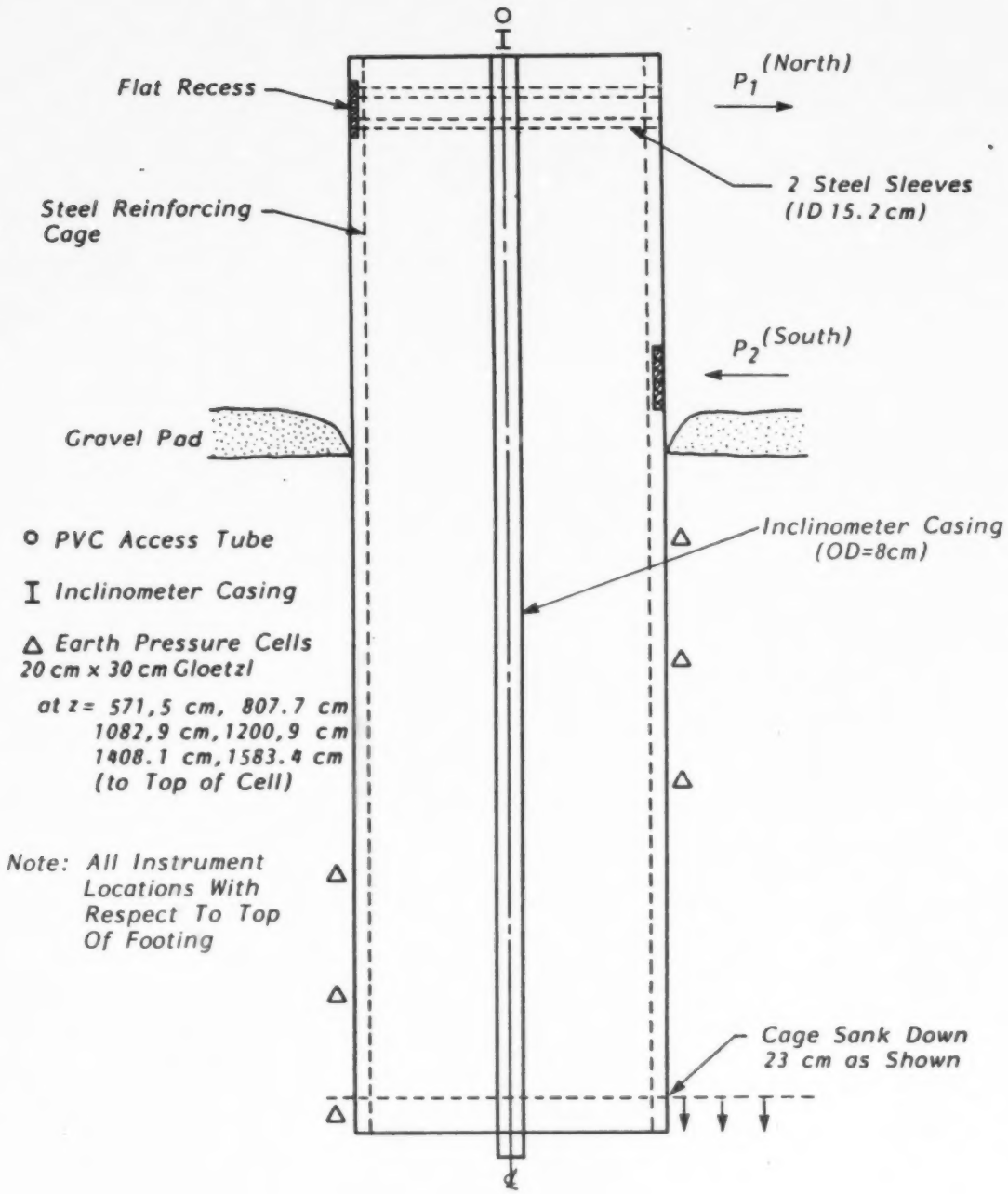

FIGURE A4

INSTRUMENTATION OF TEST FOOTING #8

2.76 m Average Diameter x 12.73 m Embedded Length

APPENDIX B

Recorded Field Data

TABLE B1

TEST NO 8
LATERAL LOAD TEST BETWEEN FOOTING #1 AND #2

Load (kN)		Horizontal Displacement, mm	
		Footing #1	Footing #2
		Footing Diameter: 0.92 m Installed Depth: 9.65 m	Footing Diameter: 1.50 m Installed Depth: 6.40 m
0		0	0
40		0.69	0.76
75	Start	1.60	1.78
	10 minute hold	2.11	2.64
130		3.40	4.34
155		4.75	6.15
200		7.37	9.53
240	Start	13.21	12.07
	10 minute hold	16.84	14.17
285		21.08	16.13
335	Start	27.69	19.18
	7 minute hold	33.73	21.34
370	Start	37.08	24.38
	7 minute hold	42.42	25.53
425	Start	59.69	30.73
355	1 hour and 35 minute hold	-	35.69
			34.80
284			28.96
150			6.10
0			

TABLE B2

TEST NO 6
LATERAL LOAD TEST BETWEEN FOOTING #2 AND #3

Load (kN)		Horizontal Displacement, mm	
		Footing #2	Footing #3
		Footing Diameter: 1.50 m Installed Depth: 6.40 m	Footing Diameter: 1.50 m Installed Depth: 6.40 m
0		0	0
45		0.36	0.36
80	18 minute hold	0.79 -> 0.66	1.09 -> 1.93
135		1.07	2.82
175	11 minute hold	1.75 -> 2.26	4.14 -> 5.54
215		2.77	6.43
260	15 minute hold	3.81 -> 4.60	8.31 -> 11.05
295		5.18	12.09
345	10 minute hold	6.30 -> 7.98	14.55 -> 17.37
380		8.87	18.75
425	10 and 20 minute hold	10.74 -> 13.06 -> 13.95	22.30 -> 26.06 -> 27.03
450		14.58	28.14
505	10 minute hold	18.01 -> 25.32	33.73 -> 42.62
55		26.90	43.89
580	10 minute hold	32.49 -> 41.63	50.24 -> 61.16
510	1 hr and 48 minute hold	41.40	63.70
345		39.60	63.63
170		35.28	59.13
0		23.34	45.03

TABLE B3

TEST NO 10a

OVERTURNING MOMENT TEST BETWEEN FOOTINGS #7 AND #8

Resultant Shear Load (kN)		Resultant Moment kN m	Eccentricities (m)	Horizontal Displacement, mm	
				Footing #7	Footing #8
				Footing Diameter: 1.60 m	Footing Diameter: 2.76 m
				Installed Depth: 6.93 m	Installed Depth: 12.73 m
0		0		0	0
5		145	29	0.69	0.20
10		240	24	0.97	0.31
15		360	24	1.07	0.46
15		480	32	1.35	0.53
20		600	30	1.47	0.53
25		725	29	1.50	0.53
30		845	28	1.12	0.51
30		965	32	1.45	0.51
40		1085	27	1.63	0.56
45		1205	27	2.01	0.69
45		1325	29	2.08	0.66
50		1450	29	2.31	0.71
55		1685	30	3.18	0.91
60		1925	32	4.50	1.12
75		2170	29	5.51	1.17
105		2410	24	7.26	1.40
150		2545	17	7.85	1.47
195	Start	2665	14	10.95	2.03
	13 minutes			15.57	2.18
285	Start	2920	10	22.63	2.82
	13 minutes			25.32	2.85
375		3175	8.5	26.24	2.87
375	(unloading)	3175	8.5	26.70	2.85
105	(unloading)	2410	24	25.63	-
45	(unloading)	1325	27	22.63	-
0		0	0	12.42	1.50
45				25.65	-
105				38.25	-
45				31.50	-
0				20.22	-

TABLE B4

TEST NO 10b (Bottom Jack removed)
OVERTURNING MOMENT TEST BETWEEN FOOTINGS #7 AND #8

Resultant & Shear Load (kN)		Resultant Moment* (kN m)	Horizontal Displacement, mm	
			Footing #7	Footing #8
			Footing Diameter: 1.60 m	Footing Diameter: 2.76 m
			Installed Depth: 6.93 m	Installed Depth: 12.73 m
0		0	0	0
90		255	1.30	0.23
180		515	5.13	0.69
265		755	9.75	1.14
310	Start	885	12.40	1.40
	4 minutes	1010	13.13	-
355	Start		15.60	1.80
	7 minutes	1140	16.84	-
400	Start		18.36	2.06
	12 minutes	1270	19.96	-
445	Start		21.39	2.41
	6 minutes	1575	22.66	-
535	Start		29.64	3.28
	15 minutes	1655	39.68	3.76
580	Start		44.50	4.34
	15 minutes	1780	60.27	4.93
625	Start		65.46	5.33
	15 minutes		-	5.97
	30 minutes		-	6.27
415		1180	-	5.79
265		755	-	4.93
90		255	-	3.71
0			-	2.29

For resultant moment multiply the resultant shear load by moment arm of 2.85 m.

TABLE B5

TEST NO 11
OVERTURNING MOMENT TEST BETWEEN FOOTINGS #6 AND #8
(with top and bottom jacks)

Resultant Shear Load (kN)	Resultant Moment (kN m)	Horizontal Displacement, mm	
		Footing #6	Footing #8
		Footing Diameter: 2.49 m	Footing Diameter: 2.76 m
		Installed Depth: 6.63 m	Installed Depth: 12.73 m
0	0	0	0
40	525	1.27	0.89
40	940	2.74	1.96
75	1460	3.10	2.11
110	1985	4.17	2.46
110	2385	4.85	2.46
135	2790	7.90	3.30
170	3375	8.51	3.43
165	3570	9.65	4.22
180	3815	10.54	4.39
165	3990	11.02	4.29
180	4235	11.56	4.37
180	4440	15.90	5.64
200	4710	20.14	5.13
155	4905	20.83	4.93
200	5130	22.84	5.36
180	5330	25.58	5.33

$\bar{e}$ (average eccentricity) = 22.90 m

TABLE B6

TEST NO 12
OVERTURNING MOMENT TEST BETWEEN FOOTINGS #6 AND #8
WITH TOP JACKS ONLY

Lateral Load P_2 From Ftg #7* (kN)	Top Load P_1 (kN)	Tie-Back** Load to Ftg #9,10,11 (kN)	Resultant Load on Footing #8 Shear (kN)	Resultant Load on Footing #8 Moment (kN m)	Horizontal Displacement, mm Footing #6 Footing Diameter: 2.49 m Installed Depth: 6.63 m	Horizontal Displacement, mm Footing #8 Footing Diameter: 2.76 m Installed Depth: 12.73 m
0	0	0	0	0	0	0
90	0	100	90	20		0.36
180	0	100	180	35		1.02
265	0	100	265	55		1.63
355	0	100	355	70		2.62
355	215	185	560	635	6.99	3.76
310	465	455	775	1285	17.81	6.35
260	590	630	850	1605	26.87	13.59
190 Start	750	800	940	2010	35.13	16.64
265 (17 min hold)	750	800	1015	2025	-	23.37
100	1120	1210	1220	2965	-	37.85
0	0	-			27.51	23.88

* Additional Lateral Load was applied to Footing #8 at ground level reacting against Footing #7.

** Footing #6, which acted as a Reaction, was tied to Footings #9, 10 and 11 at ground level (see Figure 31).

Resultant moment = $P_1e_1 + P_2e_2$

$e_1 = 2.63$ m
$e_2 = 0.20$ m

DISTRIBUTION

Mr. B.A. Oliver	Design and Development, H9A27
Mr. A.R. Collins	Design and Development, H9A23
Dr. M.S. Nashid	Design and Development, H9D24
Dr. T.W. Klym/Mr. T.J. Carmichael	Civil Research
Dr. H.S. Radhakrishna	Civil Research
Mr. R. Tsang	Civil Research

Section File (1) KR252
Public Reference Centre
Editorial Section (2)
Office Copies
Extra Copies